Cite this : New Carbon Materials, 2024, 39(2): 201-222 **DOI:** 10.1016/S1872-5805(24)60838-3

A review of the use of metal oxide/carbon composite materials to inhibit the shuttle effect in lithium-sulfur batteries

ZHOU Zhi-qiang, WANG Hui-min, YANG Lu-bin, MA Cheng, WANG Ji-tong*, QIAO Wen-ming, LING Li-cheng*

(*State Key Laboratory of Chemical Engineering, East China University of Science and Technology, Shanghai* 200237, *China*)

Abstract: Lithium-sulfur (Li-S) batteries are among the most promising next-generation electrochemical energy-storage systems due to their exceptional theoretical specific capacity, inexpensive production cost and environmental friendliness. However, the poor conductivity of S and Li_2S, severe lithium polysulfide (LiPS) shuttling and the sluggish redox kinetics of the phase transformation greatly hinder their commercialization. Carbonaceous materials could be potentially useful in Li-S batteries to tackle these problems with their high specific surface area to host LiPSs and sulfur and excellent electrical conductivity to increase electron transfer rate. However, non-polar carbon materials are unable to interact closely with the highly polar polysulfides, resulting in a low sulfur utilization and a serious shuttle effect. Because of their advantages of strong polarity and a large number of adsorption sites, integrating transition metal oxides (TMOs) with carbon-based materials (CMs) increases the chemical adsorption of LiPSs and electrochemical reaction activity for LiPSs. The working principles and main challenges of Li-S batteries are discussed followed by a review of recent research on the ex-situ and in-situ synthesis of TMO/CM composites. The formation of TMO/CMs with the dimensionalities of CMs from 1D to 3D are then reviewed together with ways of changing their structure, including heterostructure design, vacancy engineering and facet manipulation. Finally, the outlook for using TMO/CMs in Li-S batteries is considered.

Key words: Transition metal oxides; Carbon materials; Modulation strategies; Shuttle effect; Lithium-sulfur batteries

1 Introduction

To alleviate the increasingly serious pollution caused by fossil fuels and cope with the rising demand for energy sources, the need for developing novel energy-storage systems has become more urgent than ever. Traditional LIBs (LIBs) have been widely applied in various fields such as daily transportation, routine work and social communication. However, lithium iron phosphate and ternary polymer commonly used in commercial LIBs have gradually approached their upper theoretical capacity[1]. Therefore, as the requirement for electrochemical energy storage devices continues to increase, LIBs are finding it increasingly difficult to satisfy the practical demands due to their relatively low energy density.

Lithium-Sulfur (Li-S) batteries are established as one of the most promising candidates in the next-generation energy-storage systems due to merits of abundant natural reserves of sulfur, higher theory capacity (1 675 mAh g^{-1}) and longer cycling life compared with commercial LIBs[2]. Therefore, Li-S batteries have received considerable attention in the past few decades. However, numerous serious problems remain to be solved, such as the poor conductivity of S and Li_2S, severe shuttle effect of LiPSs intermediates, huge volume change of the electrode during the charge and discharge process, which greatly diminish the achievable capacity performance and lifespan of Li-S batteries.

Carbon-based materials (CM), such as carbon nanospheres, carbon nanotubes and graphene, are the most excellent conductive substrates widely used in the design and synthesis of Li-S batteries cathode composites or modified separators because of their structural diversity, large specific surface area and

Received date: 2023-10-24; **Revised date:** 2023-12-27

Corresponding author: WANG Ji-tong, Professor. E-mail: wangjt@ecust.edu.cn;
LING Li-cheng, Professor. E-mail: lchling@ecust.edu.cn

Author introduction: ZHOU Zhi-qiang, Ph.D. E-mail: zhouzhiqianggood@163.com

Homepage: http://xxtcl.sxicc.ac.cn/

outstanding electrical conductivity. Well-designed porous structure and superb electron/ion transport channels provided by CM can effectively enhance the overall conductivity and alleviate the volume expansion of active substances during repeated cycling process[3–5]. However, the weak van der Waals interaction with LiPSs of intrinsic non-polar carbonaceous materials results in a massive loss of active substances and serious shuttle effect. Among various polar metal compounds, metal oxides possess the advantages of strong polarity and abundant adsorption sites, but most of them are generally difficult to be used as substrate materials alone due to their insufficient electrical conductivity and limited porous structure[6–7]. Therefore, metal oxides are often composited with carbon materials to form TMOs-CM in the research of active materials in Li-S chemistry, contributing to increased electronic conductivity and highly exposed active sites. Additionally, it is universally acknowledged that the excellent adsorption and rapid conversion ability are two equally important factors for the “adsorption-diffusion-conversion” process in Li-S batteries. Although metal oxides supported on the carbon substrate have a strong affinity for LiPSs, the sluggish catalytic redox kinetics of trapped LiPSs results in poor electrochemical performance of TMOs-CM, especially under a high sulfur loading and a low *E*/*S* ratio. For these reasons, the modulation strategies such as heterostructures design, vacancies engineering and facet manipulation can be employed by tuning the electronic structure and constructing interfaces to greatly improve the electrochemical properties of TMOs-CM and significantly promote the catalytic conversion for LiPSs intermediates. In this review, the principles and primary challenges of Li-S batteries are firstly introduced. Then the synthesis methods and recent research advances of TMOs-CM in the past few years are presented in terms of various dimensionalities (1D, 2D, 3D). Moreover, the heterostructure design, vacancy engineering and facet manipulation of TMOs-CM composites are reviewed in detail. Finally, based on the recent achievements of TMOs-CM electrocatalysts, the conclusion and outlook are discussed to achieve the lofty goal of industrializing Li-S batteries (Fig. 1).

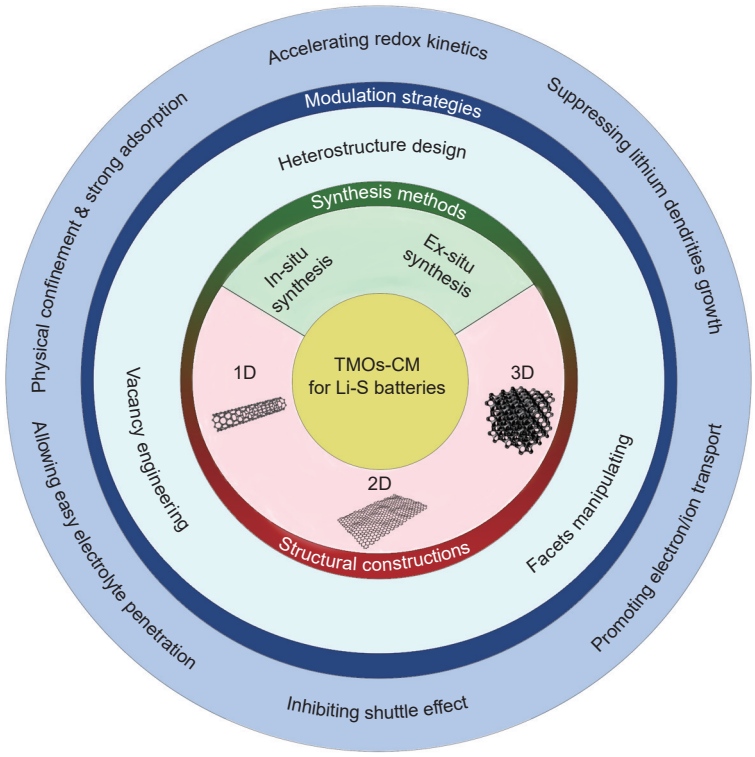

Fig. 1 Schematic illustration of synthesis methods, structural constructions and modulation strategies for TMOs-CM

2　Principles and main challenges in Li-S batteries

Different from the ion-insertion charge storage mechanism of LIBs, a multistep and reversible reaction between S_8 and lithium occurs in Li-S system during the charge-discharge process[8]. As illustrated in Fig. 2, during the discharge process, the solid-state sulfur is initially reduced to long-chain soluble LiPSs (S_8^{2-}, S_6^{2-}, S_4^{2-}) at 2.3 V, which are further reduced to highly insulating Li_2S_2 and Li_2S at 2.1 V. Reversibly, during the charge process, solid-state Li_2S and Li_2S_2 species are re-oxidized to long-chain LiPSs, which are eventually converted to sulfur through multiphase conversion. Noteworthy, the liquid-solid transformation process at 2.1 V contributes to 75% of the total specific capacity in Li-S batteries. However, the severe shuttle effect and sluggish reaction kinetics of liquid-solid conversion process during this stage leads to a significant decrease in the utilization rate of active substances, which seriously influences the electrochemical performance of Li-S batteries[9].

Despite the obvious merits of high specific capacity, low cost of active sulfur and mild environmental pollution, some inherent drawbacks present a detrimental effect on the electrocatalytic ability, including low conductivity of sulfur and short-chain polysulfides, severe shuttle effect and huge volume expansion.

Shuttle effect is one of the major problems which leads to a low sulfur utilization and severe capacity decay during the charge and discharge process[10–11]. According to the above-mentioned complicated multistep reaction process, the soluble intermediates including Li_2S_8, Li_2S_6 and Li_2S_4 with high mobility diffuse through the separator from cathode to anode during the cycle due to the concentration difference. As a result, non-uniform deposition of insoluble and insulating Li_2S are produced on the anodic surface by the migrated LiPSs, which will not only lead to severe corrosion of lithium metal, but also increase the Li^+ transmission resistance between the anode and the electrolyte. During the charge process, the formed polysulfides tend to migrate back to the cathode and are subsequently re-oxidized to the long-chain polysulfides, resulting in a low Coulombic efficiency and a severe capacity decay[12–13]. Moreover, the repeated deposition and dissolution of Li_2S will inevitably lead to the massive loss of sulfur species and the destruction of structural integrity of electrode material. In this case, enhancing the adsorption ability and boosting the sluggish redox kinetics of LiPSs intermediates are essential to inhibit the polysulfides shuttling and improve the electrochemical performance for Li-S batteries.

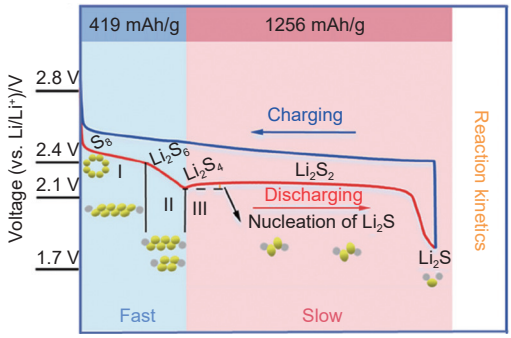

Fig. 2　Typical charge/discharge curve and multi-phase evolution of LiPSs in Li-S batteries[8]. Reproduced with permission

Volume expansion is another problem during charge and discharge process. Due to the remarkable density difference between S and Li_2S, a huge volume expansion of 80% will inevitably occur during repeated cycling which causes a low utilization rate of active sulfur species and an irreversible destruction of the structure[14–15]. In this case, with a destructed cathode integrity, the detached sulfur species lose effective electrical contact with conductive agents, which will further cause large polarization and low sulfur utilization. Therefore, electrode configuration is often well-designed to provide a certain pore volume to alleviate volume expansion of sulfur species and maintain structural stability of the cathode.

The low conductivity of both sulfur and Li_2S is the third problem which results in slow electron transfer rate and sluggish redox kinetics[16–17]. Specifically, insulating Li_2S generated during the charge and discharge process is continuously deposited on the surface of electrode, which may block the access of electrons and Li^+, cover the active sites provided by the designed materials and seriously constrain the reac-

tion kinetics process. In order to improve the utilization rate of sulfur species, composite materials are always designed to realize a uniform distribution of sulfur, good electrical contact with conductive substrate and strong adsorption-conversion ability via the addition of various electrocatalysts.

3 Synthesis methods and structural constructions of TMOs-CM

3.1 Synthesis methods of TMOs-CM

Over the past few decades, considerable efforts have been devoted to preparing electrocatalysts with active species supported on carbon-based materials of various dimensions and nanostructures to enhance the electrical/ionic conductivity of electrodes and inhibit the severe polysulfides shuttling. Among these composite materials, integrating TMOs with CM by different synthesis strategies has proved desirable for electrochemical performance in Li-S batteries. In this section, the methods for synthesizing TMOs-CM composites are divided into ex-situ and in-situ strategies, which will be discussed in detail.

3.1.1 Ex-situ synthesis

Ex-situ synthesis primarily concerns the fabrication of desired active materials beforehand, which are then encapsulated or grafted onto the surface of carbonaceous materials via covalent or non-covalent interactions[18]. In order to effectively increase the binding ability between metal catalysts and carbon supports, strong oxidants, such as HNO_3, H_2SO_4, etc., are generally employed to modify carbonaceous materials with some polar groups[19–21]. For example, graphene oxide can act as an excellent substrate to integrate with other materials through electrostatic interactions due to its abundant oxygen-containing functional groups, and can be easily transformed into reduced graphene oxide (rGO) by subsequent pyrolysis treatment without altering its original nanostructure[22]. On this basis, a VO_2@rGO composite was prepared by attaching VO_2 onto the surface of graphene oxide with large amounts of oxygen-containing groups[23]. In another case, Fe-based metal-organic framework was modified with positively charged PDDA and was easily assembled with negatively charged graphene oxide. Subsequently Fe_3O_4/NG/G was obtained by heat treatment while maintaining its highly ordered structure[24].

3.1.2 In-situ synthesis

In-situ synthesis strategies for TMOs-CM composites have been extensively researched in Li-S system, which mainly enable the nucleation and growth of active materials on the carbon-based substrate. And then TMOs-CM are produced through subsequent calcination process with ideal composition and structure, including nanotubes, nanocages, nanospheres, nanoflowers, nanosheets, etc.

Various chemical and physical synthesis technologies, such as solvothermal process[25], co-precipitation method[26], template method[27–28], sol-gel treatment[29], atomic layer deposition method[30–31], etc., have been employed for in-situ strategies. In the literatures, hydrothermal and solvothermal processes are one of the most commonly used synthesis methods since the catalysts can be well crystallized onto the surface of carbon supports resulting in remarkably enhanced active surface[32]. Recently, we demonstrated that ultra-small MnO_x-CeO_2 solid solution nanoparticles could be successfully precipitated and crystallized in the mesopores of reduced graphene oxide by a facile hydrothermal method using urea as the precipitant, which promoted the adsorption of LiPSs intermediates and boosted the precipitation and conversion of Li_2S as an advanced functional separator[33]. In another case, Ni et al.[34] reported that 1D WO_3 nanowires were encapsulated into the reduced graphene oxide in situ through hydrothermal approach. The as-synthesized rGO@WO_3 with unique 3D interconnected network not only possessed fast electron transport and Li^+ diffusion channels between sulfur and host materials, but also contributed to promoting redox reaction kinetics and mitigating the shuttle effect. Using the electrospinning method followed by subsequent high temperature treatment, the polar MnO nanoparticles were well distributed in the multichannel carbon nanofibers by Chen et al[35]. The external cross-linked carbon nanofibers and internal

multichannel structure provided sufficient electrocatalytic sites to inhibit LiPSs diffusion. It is expected that the above-mentioned in-situ methods could be further extended to the design of other various ideal TMOs-CM composites with desired structures in the future.

In-situ growth of carbon materials on as-prepared metal oxide is also a feasible method by combining the merits of carbonaceous materials and metal oxides, which not only ensures good structural stability and excellent mechanical properties of the desired structures, but also offers large SSA and improves the overall electrical conductivity. CVD method has been commonly employed for in-situ generation of carbon materials on the surfaces of different metal oxides. For example, Yang et al.[36] fabricated ZnO nanoparticles which were uniformly wrapped by ultrathin graphene-like carbon shells through CVD process by employing pyridine as carbon and nitrogen source. Benefiting from the hollow 3D structure and well-distributed ZnO nanoparticles, excellent structural stability, good electrical conductivity, and strong chemical adsorption for LiPSs could be achieved, resulting in synergistic enhancement of electrochemical performance for Li-S batteries. In another case, Luo et al.[37] synthesized V_2O_3@N,Ni-C hollow spheres through CVD process by using octadecyl amine as carbon source. Compared with pure V_2O_3, the hollow spherical structure composed of numerous nanosheets on the surfaces of V_2O_3@N,Ni-C was conducive to the diffusion of lithium ion and the buffering of volume expansion during the electrochemical processes, leading to improvement of redox conversion of polysulfides.

3.2 Structural constructions of TMOs-CM

Carbon-based materials derived from biomass[38–39], carbon nanotubes[40], graphene oxides[41] and metal-organic frameworks[42] have been introduced as excellent substrates for the nucleation of metal oxides. As for the typical TMOs-CM composite materials, metal oxides tend to alleviate the shuttle effect through their ability to adsorb LiPSs while carbon materials can enhance the overall conductivity and buffer the volume expansion through their easily adjustable structure. In recent years, diverse morphological structures of TMOs-CM, including one-dimension (1D), two-dimension (2D) and three-dimension (3D), have been extensively applied in the fields of Li-S batteries. In this section, the characteristics and application of TMOs-CM with different dimensionalities will be introduced in detail.

3.2.1 1D TMOs-CM

During the synthesis of 1D composite materials, carbon nanotubes (CNTs) have been considered as highly promising carbon supports to integrate with metal oxides due to superior long-range conductivity and rigid structural properties. For 1D TMOs-CM, the contact area between active material and LiPSs is greatly improved and the formed interconnected network can greatly enhance the overall electrical/ionic conductivity[43]. For example, Choi et al.[44] developed a novel electrical wire explosion process to uniformly embed polar MoO_2 nanoparticles onto conductive CNT scaffolds as multifunctional separator for Li-S batteries (Fig. 3a). As presented in Fig. 3b-e, MoO_2 nanoparticles were well-dispersed in the CNTs scaffolds and abundant vacant voids were detected in MoO_2@CNT, which enhanced the contact area with LiPSs and promoted the chemical affinity for LiPSs of polar MoO_2. Meanwhile, conductive CNT scaffold as a conductive substrate could enhance the overall electrical conductivity and physically block LiPSs intermediates. Therefore, MoO_2@CNT with an appropriate compositional ratio exhibited a low-capacity decay rate of 0.398% per cycle at 0.2 C and a high specific capacity of 540 mAh g^{-1} at 1 C after 700 cycles with a low-capacity decay rate of 0.066% per cycle. In another case, Yao et al.[45] proposed a simple strategy to synthesize Co-SnO_2@CNT nanocomposites by a facile hydrolysis process and a subsequent calcination treatment. Due to the advantages of excellent electrical conductivity of CNTs, chemical adsorption ability of SnO_2 and catalytic ability of Co, the cathode material could significantly alleviate the polysulfides shuttling and promote the redox ability of trapped LiPSs. As a result, the assembled batteries presented a stable capability of 710 mAh g^{-1} over 600 cycles at 1 C with a capacity decay rate of 0.042% per cycle. In another

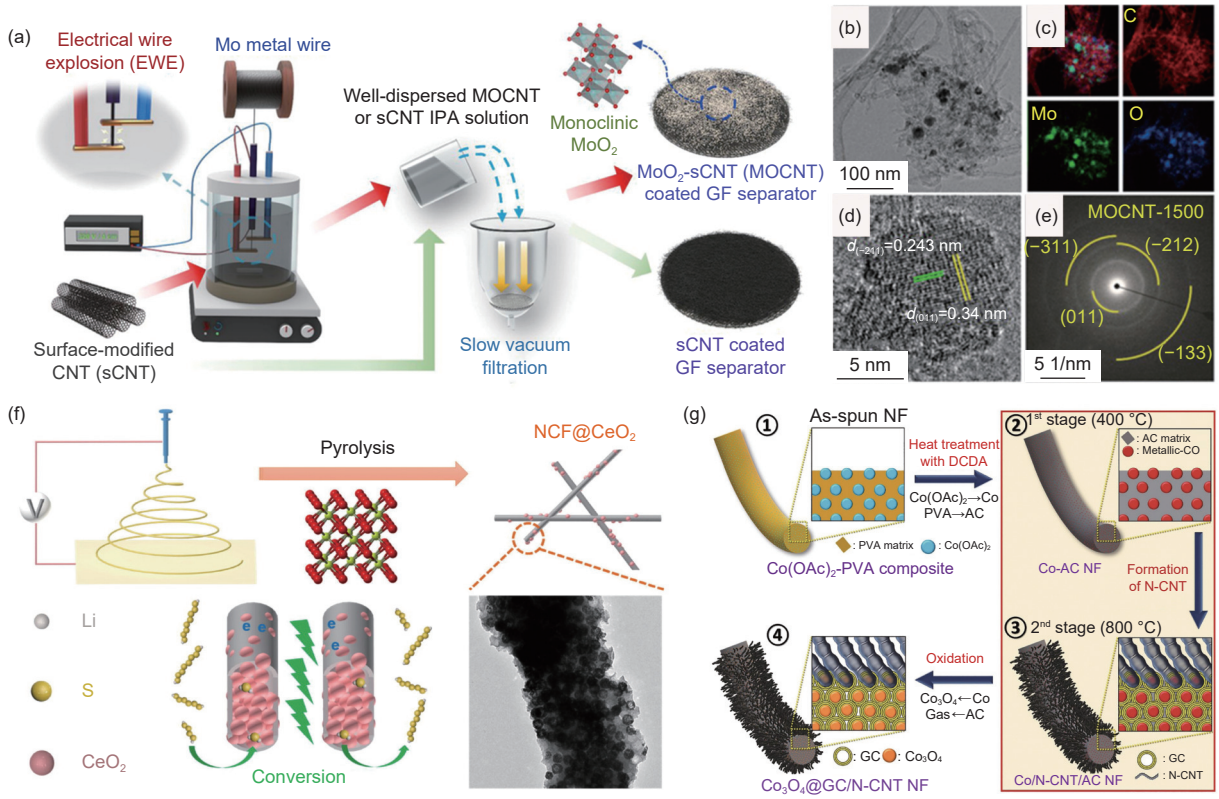

Fig. 3 (a) Schematic synthesis of MoO_2@CNT nanocomposites[44]. (b-e) SEM and TEM images of MoO_2@CNT[44]. (f) Schematic synthesis of NCF@CeO_2 interlayer[47]. (g) Schematic illustration of the formation procecss of core-shell Co_3O_4@GC/N-CNT NF[48]. Reproduced with permission

work, Qiu et al.[46] fabricated a TiO_2/Co_3O_4-CNTs composite derived from MIL-25(Ti) as a cathode material for Li-S batteries. During the preparation process, Co_3O_4 nanoparticles were deposited into the TiO_2 structure and the CNTs were vertically produced on the surface of TiO_2/Co_3O_4 through CVD method. Due to the merits of porous structure of conductive CNT matrix and strong affinity for LiPSs of polar TiO_2/Co_3O_4, the TiO_2/Co_3O_4-CNF cathode could maintain a capacity decay rate of 0.097% over 500 cycles at 0.5 C.

Apart from nanotubes, 1D nanofibers have also achieved widespread attention in Li-S systems. As for the synthesis methods, electrospinning technology has proved to be an effective approach to fabricate 1D nanofibers with embedded polar TMOs. In a recent work, Wen et al.[47] fabricated a multifunctional nanofiber with CeO_2 spheres embedded in nitrogen-doped carbon nanofiber (NCF) by an electrospinning technique, which was employed as an interlayer in Li-S batteries. The skeleton matrix provided by 1D NCF served as a conductive channel to promote interfacial electron transfer (Fig. 3f). Moreover, the hollow structure of CeO_2 spheres with rich oxygen defects could strongly trap LiPSs and ensure efficient catalytic conversion. Profiting from the “sphere-in-fiber” structure and abundant active sites, NCF@CeO_2 interlayers presented a capacity decay rate of 0.063% per cycle after 1 000 cycles at 1 C. In another case, Saroha et al.[48] proposed a hierarchically fibrous structure named Co_3O_4@GC/N-CNT NF. During the synthesis process, highly conductive CNTs could be generated through the reaction between metallic cobalt and CH_x gas produced by DCDA (Fig. 3g). Moreover, CNTs and nanofibers ensured the excellent electrical conductivity and rapid ionic transfer of the interlayer composite material, while Co_3O_4 nanoparticles with numerous polar sites could effectively capture the soluble polysulfides. Consequently, the cell with the Co_3O_4@GC/N-CNT NF interlayer showed a capacity decay rate of 0.040% per cycle over 900 cycles at 0.1 C.

3.2.2 2D TMOs-CM

During the synthesis process of 2D TMOs-CM,

the generation of 2D carbon layer can restrain the agglomeration of TMOs and make them uniformly distribute on the surface of carbon materials after calcination. Therefore, 2D conductive carbon materials can provide rapid charge transfer and realize high utilization of active materials, while the embedded TMOs can expose abundant catalytic sites, which are beneficial to the suppression of LiPSs shuttling.

Graphene and their derivatives have been widely employed as efficient sulfur hosts with strong physical confinement of LiPSs due to ultrahigh specific surface area, excellent electrical conductivity and outstanding mechanical/chemical properties[49]. Higher sulfur loading and sulfur utilization can be achieved since sulfur can be uniformly distributed on graphene nanosheets. Therefore, through cooperation of graphene nanosheets and transition metal oxides, superior electrochemical performance can be achieved. On this basis, He et al.[50] proposed a multifunctional flower-like $CoTiO_3$ wrapped by rGO as an efficient sulfur immobilizer by a hydrothermal method, as displayed in Fig. 4a. Specifically, rGO wrapped on $CoTiO_3$ spheres could provide a highly conductive network for fast electronic and ionic transfer. Meanwhile, a high sulfur loading was realized by the hollow structure in the composite material. Therefore, the integration of physical structure and chemical composition endowed the $CoTiO_3$@rGO with strong adsorption and fast catalytic kinetics for LiPSs. As a result, the assembled batteries presented superior cycling stability with a capacity fading of 0.013% per cycle after 500 cycles at 1 C and retained an area capacity of 5.02 mAh cm^{-2} under a high S loading of 5.2 mg cm^{-2}. In another work, Qiu et al.[51] achieved in-situ synthesis of ultra-small MnO clusters which were incorporated into 2D ordered mesoporous carbon nanosheets. As shown in Fig. 4b-e, the abundant mesoporous tunnels on both sides of rGO nanosheets

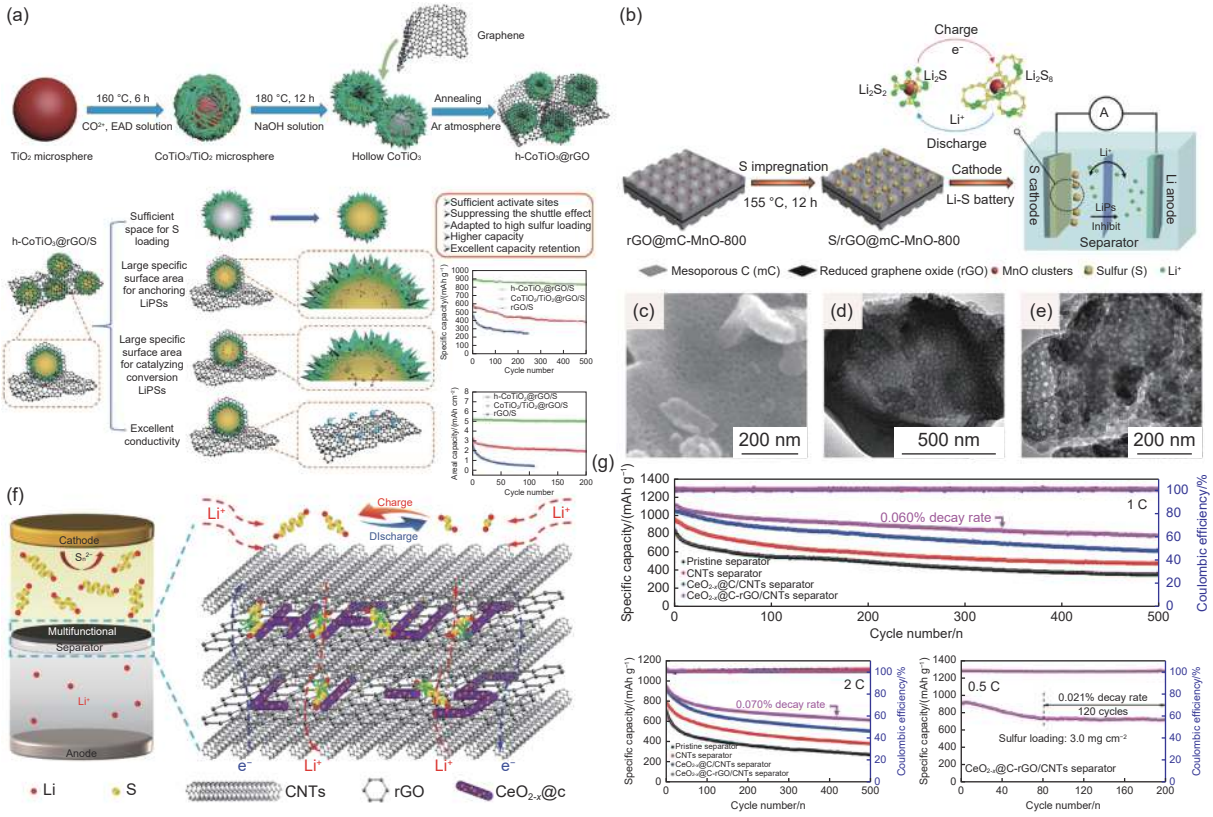

Fig. 4　(a) Schematic illustration of preparation process of $CoTiO_3$@rGO and synergistic functions in Li-S batteries[50]. (b) Schematic electrode configuration of Li-S batteries with S/rGO@mC-MnO-800 cathode material[51]. (c) SEM image of S/rGO@mC-MnO-800 cathode material[51]. (d, e) TEM images of S/rGO@mC-MnO-800 cathode material[51]. (f) Diagram of configuration of Li-S batteries with CeO_{2-x}@C-rGO/CNTs separator[52]. (g) Cycling behavior at 1 C, 2 C, 0.5 C respectively[52]. Reproduced with permission

could provide conductive channels for electron transfer and exert an effective buffering impact for volume expansion. According to DFT calculations, the higher adsorption energy of LiPSs on MnO clusters proved that MnO could efficiently stabilize the LiPSs to alleviate the shuttle effect. Benefiting from the delicate design, the batteries presented reversible performances of 684 mAh g^{-1} after 250 cycles at 2 A g^{-1} and a superior rate capability of 808 mAh g^{-1} at 4 A g^{-1}.

Besides, rational cooperation of 2D nanosheets with other nanostructured materials of different dimensionalities is considered as an effective approach to boost the electrochemical performance of Li-S batteries, which synergize structural advantages and multi-functionalities of catalytic properties together. For example, Li et al.[52] prepared a multifunctional multilayered CeO_{2-x}@C-rGO/CNT separator via coating CNTs and CeO_{2-x}@C-rGO layers on a commercial separator. Owing to the synergy of CeO_{2-x}@C with high catalytic ability and rGO/ CNTs with superior electronic conductivity, the modified separator could chemically restrain the diffusion of LiPSs, and promote the redox reactions of sulfur species. Therefore, the modified separator demonstrated a capacity decay rate of 0.060% per cycle over 500 cycles at 1 C and 0.070% per cycle over 500 cycles at 2 C. Moreover, under a sulfur loading of 3 mg cm^{-2}, a capacity decay rate of 0.021% was achieved after 120 cycles at 0.5 C (Fig. 4f-g). In recent years, quantum-dot materials with a sub-10 nm size have received extensive interest in Li-S batteries, including ZnO[53], SnO_2[54] and TiO_2[55]. However, the serious aggregation of quantum dots (QDs) due to their high surface energy results in poor cycle stability and rate performance. One of the effective solutions is to integrate ultrasmall QDs materials with 1D, 2D or 3D carbonaceous materials. The as-prepared composite materials can alleviate the aggregation of quantum dots, help accelerate the electron/ion transfer, and improve the catalytic conversion for Li-S batteries. In a recent work, Zhang et al.[56] designed Ti_nO_{2n-1} QDs which were well dispersed on 2D porous carbon nanosheet (OV-T_nQDs@PCN) as sulfur host. Due to the synergistic combination with OV-T_nQDs and PCN, the LiPSs were effectively trapped through strong chemical confinement. Therefore, the Li-S cell with this composite cathode delivered a specific capacity of 878 mAh g^{-1} at 0.1 C after 100 cycles and a low-capacity decay rate of 0.012% after 1 000 cycles at 2 C.

3.2.3 3D TMOs-CM

3D TMOs-CM are one of the most widely investigated composite materials for Li-S batteries, including hollow nanosphere, aerogels and arrays. Compared with typical carbon materials, such as carbon nanotubes and graphene, 3D carbon materials can be easily synthesized with a relatively low production cost. Moreover, the structure of 3D carbon supports can be well-designed with reliable sulfur accommodation, interconnected networks for fast electron/ion transfer and well-distributed porous channels for electrolyte infiltration. After integrating with TMOs, the formed 3D TMOs-CM composites can provide accessible sites for the adsorption and conversion of LiPSs, leading to desired electrochemical performance for Li-S batteries.

3.2.3.1 Hollow nanospheres

3D hollow nanosphere with hierarchically porous architecture has received intensive interest in recent years since different pore sizes present respective functions in Li-S batteries. Specifically, micropores tend to offer strong physical affinity for LiPSs and prevent the diffusion of LiPSs into the electrolyte, while interconnected mesopores and macropores can provide rapid ionic transportation, easy penetration of electrolyte and sufficient space to accommodate the volume expansion of electrode. As for the preparation process, hard templates, such as SiO_2[57–58], PMMA[59–60], and polystyrene[61–63] are frequently employed to introduce abundant pores of different sizes into the carbon materials, resulting in high specific surface area, excellent electrical conductivity and hierarchically porous structure. On this basis, Co@NCNTs/Co-TiO_2 composite material was designed with Co@NCNTs grown in situ into the 3DOM architecture of Co-TiO_2[62] Due to synergistic effects of the excellent conductivity of NCNTs, strong

adsorption ability of Co-TiO_2 and remarkable catalytic activity of Co nanoparticles, the redox kinetics was remarkably enhanced and the growth of lithium dendrites were efficiently inhibited as shown in (Fig. 5a). As a result, the assembled batteries exhibited a capacity of 874.09 mAh g^{-1} after 500 cycles at 1 C with a low decay rate of 0.027% per cycle and a rate capacity of 624 mAh g^{-1} at 5 C.

In addition, Liu et al.[64] rationally designed a multifunctional sulfur host by in-situ encapsulating $ZnCo_2O_4$ QDs (ZCO-QDs) into the hollow carbon sphere (HCS) by a facile hydrothermal process. The conversion mechanism presented that the higher concentration of abundant $S_3^{\bullet-}$ radicals were produced by the boosted dissociation reaction of S_6^{2-} compared with QDs@HCS by in-situ UV-Vis experiment, demonstrating the efficient anchoring ability and catalytic conversion of LiPSs on the cathode side. Moreover, it was found that ZCO-QDs as self-healing materials could repair broken SEI layers and induce uniform Li deposition on the anode side (Fig. 5b). As a result, ZCO-QDs@HCS cathode material obtained a rate capability of 595.5 mAh g^{-1} at 5 C and a capacity of 675.2 mAh g^{-1} with a decay rate of 0.083% per cycle at 1 C over 400 cycles.

In addition, TMOs-CM with well-designed 3D structures (e.g., yolk-shell structure) tend to exhibit satisfactory electrochemical performance since sulfur can be well accommodated in the interior void, while the outer rigid carbon shell maintains the structural integrity during charge and discharge process. TMOs such as VO_2 and δ-MnO_2 could produce thiosulfate surface groups ($S_2O_3^{2-}$) in-situ through oxidation of LiPSs, and then active polythionate complex ($S_xO_6^{2-}$) were formed by further catenating $S_2O_3^{2-}$ with newly formed long-chain LiPSs to inhibit polysulfides dis-

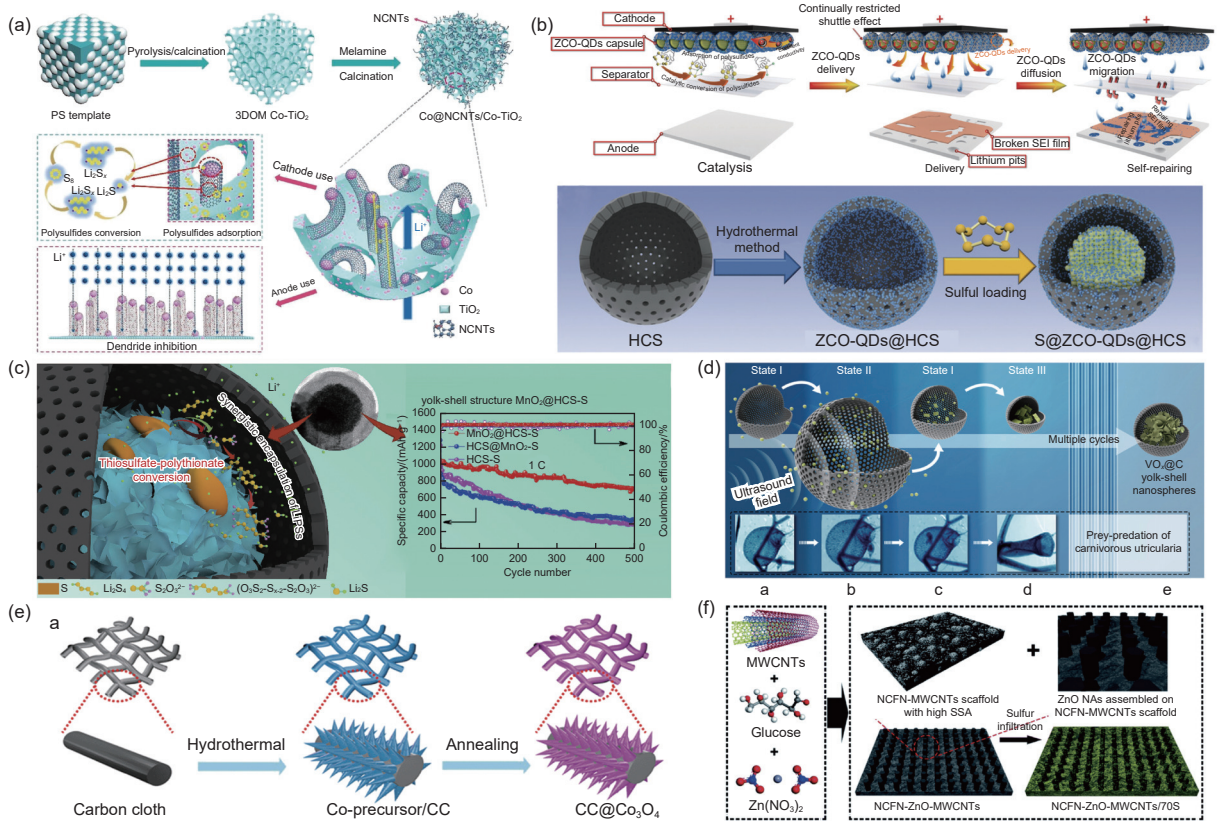

Fig. 5　(a) Schematic illustration of synthesis process and the corresponding function of Co@NCNTs/Co-TiO_2[62]. (b) Schematic diagram of polysulfides conversion process on ZCO-QDs surface[64]. (c) Schematic illustration of synergistic advantages of yolk-shell MnO_2@HCS-S and the corresponding cycling performance at 1 C[66]. (d) Synthesis route of VO_x@C yolk-shell nanospheres under high-frequency ultrasonic excitation[68]. (e) Diagram of the preparation process of the CC@Co_3O_4[71]. (f) Schematic illustration of the synthesis process of ZnO NAs assembled on NCFNs-MWCNTs scaffold[73]. Reproduced with permission

solution into the electrolyte[65]. On this basis, Shao et al.[66] developed a novel design of yolk-shell structure, in which hollow carbon nanospheres were filled with highly polar MnO_2 nanoflakes (Fig. 5c). The outer carbon shell of the MnO_2@hollow carbon nanospheres restrained the volume expansion and diffusion of soluble LiPSs by physical confinement. Besides, the inner MnO_2 nanoflakes could capture LiPSs and conduct thiosulfate-polythionate conversion to promote the redox kinetics. Benefitting from the synergistic effect of structural and chemical properties, the composite cathode presented good electrochemical performance with long-cycle stability of a capacity decay of 0.078% per cycle in 500 cycles at 1 C. In another work, Zhang et al.[67] constructed a hollow micro-mesoporous structure with hydrangea-like MnO_2 wrapped onto the surface of hollow carbon (HC) nanospheres. The designed hollow structure as a physical barrier could alleviate volume expansion and enhance the overall conductivity for Li^+ and electron transfer, while MnO_2 as a chemical electrocatalyst could efficiently anchor and convert LiPSs. Therefore, the MnO_2-HC-S cathode achieved a capacity loss of 0.039% per cycle after 1 000 cycles at 0.5 C with a sulfur loading of 1.8 mg cm^{-2}.

Different from conventional diffusion or infusion methods to construct yolk-shell structure, Ji et al.[68] pioneered the work of biomimicking the predation process of carnivorous utricularia to synthesize VO_x@C yolk-shell nanosphere as an interlayer for Li-S batteries. Specifically, VO_x nanoparticles could be well encapsulated into the hollow mesoporous carbon spheres (HMCS) under high-frequency ultrasonic excitation to form VO_x@C yolk-shell nanosphere, as shown in Fig. 5d. Besides, the core-shell structure of C@VO_x could also be obtained by adjusting sonication time. The resulting VO_x@C delivered a better capacity of 860 mAh g^{-1} after 100 cycles at 0.2 C compared with PP, CNT and C@VO_x.

3.2.3.2 Aerogels

3D graphene aerogel composed of inter- connected graphene network possesses advantages of high specific surface area, 3D electron transmission channels and superior electrical conductivity. Zhang et al.[69] proposed a two-step method to prepare a hybrid with 1D vanadium oxide (VO_x) nanorods encapsulated in graphene aerogel as an efficient physical and chemical barrier in Li-S batteries. Apart from the strong chemical anchoring ability for LiPSs, VO_x with catalytic functions could also catalyze LiPSs into thiosulfates and polysulfates. Being applied as a modified separator, the assembled batteries delivered a stable specific capacity of 441 mAh g^{-1} after 600 cycles at 1 C.

TiO_2 as a conventional metal oxide has been widely applied as the component of the composite cathode in Li-S batteries. For the integration of TiO_2 and 2D carbon substrate, anatase TiO_2 supported on the carbon materials tends to form (101) facets preferentially. However, 2D carbon materials generally expose (001) facets, which makes the composite of TiO_2 and 2D carbon material hard to integrate[70]. To address this problem, Wang et al.[70] developed a composite cathode which consisted of 3D porous graphene aerogel (GA) and anatase TiO_2 (001) nanoplates. For the synthesis process of this composite material, both TiO_2 nanoplates and graphene oxide are integrated in a $NaHSO_3$ solution. Followed by a hydrothermal approach and freeze-drying technique, TiO_2 with abundant (001) facets was highly exposed on GA. Because of the good match between the anatase TiO_2 (001) facets and the 3D porous graphene aerogel (002) facet, the cathode could immobilize the LiPSs by both physical confinement (porous structure of the graphene aerogel) and chemical confinement (chemical bind between soluble sulfurous species and TiO_2), resulting in long cycling stability.

3.2.3.3 Arrays

Carbon cloth (CC) as a conductive carbon substrate has been extensively researched because of efficient charge transport and accommodation of active materials. Besides, the 3D porous network formed by interlinked nanofibers can effectively expose active sites and allow rapid penetration of the electrolyte. Chang et al.[71] rationally developed Co_3O_4 nanoneedle arrays resembling a bottlebrush shape on car-

bon cloth fibers ($CC@Co_3O_4$) by a simple hydrothermal method (Fig. 5e). As a multifunctional "super-reservoir", the well-designed 3D array structure could accommodate the repeated precipitation and dissolution of Li_2S during the discharge and charge process. Moreover, the strong affinity for soluble LiPSs of polar Co_3O_4 nanoneedles could effectively inhibit the LiPSs shuttling and make Li_2S_2/Li_2S uniformly deposit on the surface by greatly reducing the reaction activation energy. Therefore, the freestanding $CC@Co_3O_4$ exhibited a degradation rate of 0.060% over 280 cycles at 1 C and a capacity of 476 mAh g^{-1} after 500 cycles at 2 C. Chen et al.[72] developed a freestanding $S/CC@NiCo_2O_4$ sulfur host through a simple hydrothermal reaction and a subsequent two-step annealing process. Attributed to the special 3D hierarchical structure formed by interconnected network of CC and $NiCo_2O_4$ nanofiber arrays, the exposed adsorption sites and boosted redox kinetics of LiPSs greatly improved electrochemical performance compared with CC. Specifically, the cathode showed a specific capacity of 660 mAh g^{-1} after 200 cycles at 0.2 C with a sulfur loading of 3.5 mg cm^{-2} and a capacity of 9.0 mAh cm^{-2} with a sulfur loading of 8.9 mg cm^{-2}.

In another work, Yao et al.[73] developed a facile strategy to prepare a specially ordered structure with ZnO nanoprism arrays (ZnO NAs) grown on N-doped carbon foam nanoplates-MWCNTs (NCFN-MWCNTs). As shown in Fig. 5f, ZnO nanoarrays were vertically grown and uniformly dispersed on the NCFN substrate. Moreover, NCFNs were tightly interconnected with MWCNTs to guarantee rapid electron transfer. Benefitting from the 3D interconnected conductive network with hierarchically porous structure and polar ZnO NAs with strong anchoring effect, the assembled batteries achieved a rate capacity of 506.1 mAh g^{-1} at 5 C and a decay rate of 0.035% over 2 000 cycles at 0.5 C under a sulfur loading of 5.6 mg cm^{-2}.

4 Modulation strategies

4.1 Heterostructure design

Despite remarkable progress towards structure engineering of TMOs-CM in the field of Li-S batteries (Table 1), the electrochemical performance of individual metal oxide-carbon material remains to be improved, particularly under high current densities and high sulfur loadings. In recent years, designing heterogenous interfaces has proved to be an effective

Table 1　Summary of electrochemical performance of various TMOs-CM electrocatalysts in Li-S batteries

Electrocatalyst	S loading/ (mg cm^{-2}) & content	Capacity at low current/ (mAh g^{-1})	Rate capability/ (mAh g^{-1})	Capacity at high current/ (mAh g^{-1})	Ref.
MoO_2@CNT	1.4-1.7&75%	1067 (100^{th}, 0.2 C)	369@5 C	540 (700^{th}, 1 C)	[44]
Co-SnO_2@CNT	3.0&79%	767 (400^{th}, 0.2 C)	808@2 C	710 (600^{th}, 1 C)	[45]
NCF@CeO_2	1.4&70%	–	506@4 C	315 (1000^{th}, 1 C)	[47]
Co_3O_4@GC/N-CNT NF	2.0&70%	712 (250^{th}, 0.1 C)	329@2 C	319 (900^{th}, 1 C)	[48]
$CoTiO_3$@rGO	1.2&49%	1075 (500^{th}, 0.2 C)	754@2 C	836 (500^{th}, 1 C)	[50]
OV-TnQDs@PCN	2.2&79%	878 (100^{th}, 0.1 C)	672@2 C	660 (1000^{th}, 2 C)	[56]
Co@NCNTs/Co-TiO_2	2.0&60%	1129 (100^{th}, 0.2 C)	624@5 C	874 (500^{th}, 1 C)	[62]
ZCO-QDs@HCS	1.3&70%	–	596@5 C	675 (400^{th}, 1 C)	[64]
MnO_2@HCS	1.5&63%	744 (100^{th}, 0.1 C)	765@1 C	705 (500^{th}, 1 C)	[66]
MnO_2-H C	1.8&60%	663 (200^{th}, 0.2 C) 423 (1000^{th}, 0.5 C)	621@3 C	–	[67]
VO_x@C	4.3&70%	860 (100^{th}, 0.2 C)	540@5 C	600 (200^{th}, 1 C)	[68]
GA-VO_x/CB	1.0&80%	708 (200^{th}, 0.2 C)	442@2 C	441 (600^{th}, 1 C)	[69]
$CC@Co_3O_4$	4.1&—	987(200^{th}, 0.5 C)	610@2 C	476 (500^{th}, 2 C)	[71]
V_2O_3/V_8C_7@C@G	1.2-1.5&64%	1028 (200^{th}, 0.2 C)	588@5 C	745 (1000, 1 C)	[81]
Fe_9S_{10}/Fe_3O_4@C	1.0&56%	–	660@5 C	587 (500^{th}, 1 C)	[82]
TiO_2@MoS_2	1.0-1.2&75%	902 (300^{th}, 0.5 C)	601@5 C	578 (500^{th}, 2 C)	[83]
G-m$SnO_2/SnSe_2$	1.8&64%	1341 (300^{th}, 0.2 C)	794@8 C	1016 (1000^{th}, 1 C)	[84]
GP/CNT/LNO-V	4.4&60%	962 (100^{th}, 0.2 C)	844@1 C	571 (400^{th}, 1 C)	[88]
NFBCoFe_2O_{4-x}@MWCNTs	2.0&63%	1156 (300^{th}, 0.2 C)	746@5 C	870 (1000^{th}, 1 C)	[90]
Co_3O_4-NP/N-rGO	1.0&60%	914 (100^{th}, 0.2 C)	569@3 C	608 (500^{th}, 1 C)	[94]
SnO_2 {332}-G	1.2&68%	687 (500^{th}, 0.5 C)	616@4 C	432 (2000^{th}, 2 C)	[95]

strategy to realize a smooth “adsorption-diffusion-conversion” process, which is of great significance to the accelerated redox kinetics of LiPSs and shuttle effect inhibition in Li-S batteries[74–76]. Unlike physically mixing different materials, heterostructure refers to a composite material composed of two or more types of active materials through physical (mainly van der Waals force) or chemical bonds. As illustrated in Fig. 6a, due to differences of band structures, semiconductor types and Fermi energy levels, charge distribution of catalytic materials tend to change by the ideally interior built-in electric field until the Fermi energy level reaches equilibrium, resulting in enhanced electrical conductivity, improved Li ion diffusion and highly exposed active sites[76–78]. This strategy which combines the advantages of different components can effectively achieve the synergistic effect of adsorption and catalysis function[79].

Generally, metal oxides with strong polarity like MnO_2 and VO_2 can interact with LiPSs to form thiosulfate and polysulfate species as redox media, which possess strong anchoring ability for LiPSs[80]. However, due to the inferior conductivity of single polar metal oxides and limited catalytic activity for redox kinetics of LiPSs, it is detrimental for the LiPSs conversion during long-time cycling in Li-S batteries. Therefore, it is necessary to diffuse adsorbed LiPSs from metal oxides to the nearby conductive composite surface to accomplish further LiPSs conversion. In recent years, many studies have demonstrated that metal compounds such as nitrides, sulfides, selenides and phosphides presented strong catalytic conversion ability for LiPSs. Therefore, the preparation of metal oxide-metal compound heterostructures are considered as an efficient approach to combine additional chemical adsorption sites with redox kinetics ability to achieve a smooth “adsorption-diffusion-conversion” process, which can significantly reduce the interface resistance, lower the decomposition energy barrier of Li_2S and facilitate the redox kinetics of LiPSs.

Carbonaceous nanomaterials derived from metal-organic frameworks (MOFs) have been extensively applied as emerging electrocatalysts which possess large specific surface area, highly adjustable porous structure, and excellent electrical conductivity. On this basis, Zhang et al.[81] proposed a porous

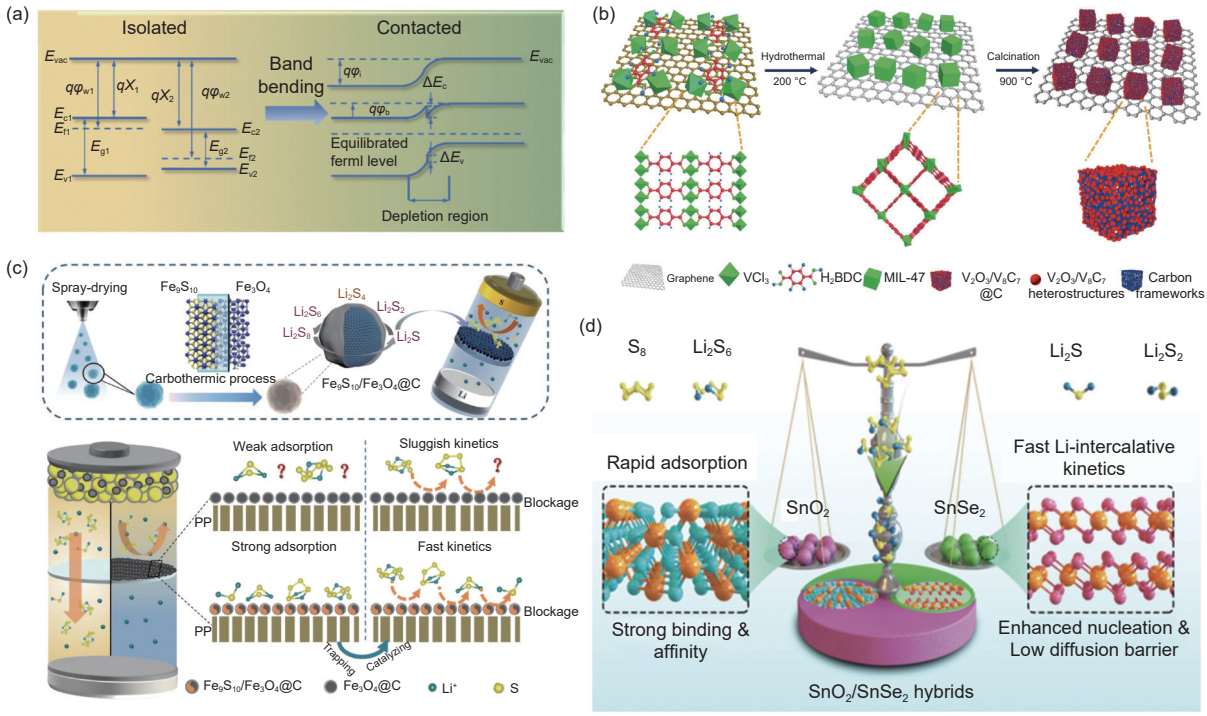

Fig. 6 (a) Diagram of formation mechanisms of heterostructures[78]. (b) Schematic illustration of the synthesis route of V_2O_3/V_8C_7@C@G heterostructure[81]. (c) Schematic illustration of the preparation process and synergistic function of Fe_9S_{10}/Fe_3O_4@C heterostructure[82]. (d) Illustration of the multifunctional interlayer on modified separator constructed by $SnO_2/SnSe_2$ heterostructure[84]

V_2O_3/V_8C_7@carbon composite heterostructure derived from MIL-47(V), as displayed in Fig. 6b. With respect to this cathode, soluble LiPSs were well anchored by V_2O_3 via strong chemical absorption and then transferred to the surface of V_8C_7 through the effective built-in interface to accomplish the efficient redox conversion from LiPSs to Li_2S. Owing to the smooth "adsorption-diffusion-conversion" process, the heterostructure presented an excellent long-term lifespan with only 0.017% capacity decay per cycle in 1 000 cycles. More critically, a superior areal capacity of 4.3 mAh cm^{-2} was achieved after 150 cycles, exceeding most cathode materials used in lithium-sulfur batteries. In a recent work, Xu et al.[82] proposed a core-shell Fe_9S_{10}/Fe_3O_4 heterostructure as an efficient cathode material, which was synthesized by a simple spray-drying technique and a subsequent in-situ carbothermal reduction method (Fig. 6c). The strong anchoring and conversion ability of polar Fe_3O_4 and conductive Fe_9S_{10} exhibited a trapping-catalyzing effect which could greatly decrease the capacity decay. Additionally, the formation of the carbon shell outside the Fe_9S_{10}/Fe_3O_4 core ensured electronic and ion conductivity of nanocomposites. Attributed to the superiorities of structural and chemical properties, the heterogeneous Fe_9S_{10}/Fe_3O_4 interlayer showed a capacity decay rate of 0.08% per cycle and a superior rate performance of 660 mAh g^{-1} at 5 C. Lee et al.[83] prepared TiO_2-MoS_2 heterostructure on carbon cloth substrate with well-controlled structure and chemical composition through a facile ALD technique and a subsequent hydrothermal process. Combining the advantages of strong LiPSs trapping ability (TiO_2) and fast redox conversion kinetics (MoS_2), the designed heterostructure with optimally oriented built-in field could synergistically induce rapid migration of LiPSs intermediates, alleviate the shuttle effect and expedite LiPSs redox kinetics. Consequently, the composites presented a rate capacity of 601 mAh g^{-1} at 5 C, and a capacity of 5.2 mAh cm^{-2} were achieved at 0.1 C after 100 cycles with a high sulfur loading of 5.2 mg cm^{-2}.

In addition to the considerable efforts devoted to the adsorption-diffusion-conversion processes on the cathode side, the heterogeneous structure also has the potential to induce uniform Li deposition due to the internal electric field at the heterogeneous interface on the anode side. 2D mesoporous SnO_2-$SnSe_2$/rGO electrocatalyst as efficient LiPSs catalytic promoter and lithium regulator synergized the merits of strong chemical affinity of SnO_2, outstanding redox ability of $SnSe_2$ and rapid conversion kinetics of Li_xSnSe_2 (Fig. 6d), thereby facilitating Li_2S nucleation and decomposition, improving the chemical adsorption with LiPSs and the overall electronic conductivity[84]. Moreover, the functional separator modified by SnO_2-$SnSe_2$/rGO with strong lithiophilic characteristics could effectively reduce the Li nucleation overpotential, and thus inducing uniform Li plating/stripping process and suppressing Li dendrite growth. Impressively, a high-rate capacity of 794 mAh g^{-1} were achieved at 8 C and an admirable capacity of 648 mAh g^{-1} over 2 000 cycles at 5 C with an extremely low-capacity decay rate of only 0.014% per cycle were shown. Based on representative studies presented above, it can be rationally concluded that heterostructures design is greatly conductive to the improvement of electrochemical performance for Li-S batteries.

4.2 Vacancy engineering

Due to the strong interaction between the O^{2-} and LiPSs, the introduction of oxygen vacancies (OVs) into metal oxides for vacancies engineering has also attracted great attention in recent years. Compared with the defect-free crystal structure with stable charge distribution, the formation of OVs can effectively regulate the electronic structure near Fermi level and intrinsic catalytic activity of metal oxides[85–86]. Rational engineering of OVs in the metal oxides can produce large amounts of active electrons and unsaturated coordination sites around defects, which improve the chemisorption and catalytic conversion of polysulfides by improving the electronic conductivity and exposing abundant active centers[87]. Therefore, the overall conductivity and redox conversion kinetics are remarkably enhanced with OVs incorporated into metal oxides.

In a recent work, CNTs and $LaNiO_{3-x}$ nanoparticles were uniformly filled into a honeycomb-like framework of graphitized pinus sylvestris (GP) as an advanced sulfur host for Li-S batteries (Fig. 7a)[88]. The existence of OVs were confirmed by the strong intensity at g=2.001 and the peak located at 530.1 eV according to EPR and XPS characterization as shown in Fig. 7b-c. In addition, theoretical calculations proved that Ni-S and La-S bonds were formed since the active electrons around OVs could make Li-S and S—S bonds easy to break, indicating a significantly stronger interaction between $LaNiO_{3-x}$ and LiPSs compared with $LaNiO_3$. Attributed to the highly ordered microchannel structure of graphitized pinus sylvestris (GP) and efficient adsorption/catalytic ability of defective $LaNiO_{3-x}$, the assembled cell presented an excellent capacity of 714 mAh g^{-1} after 500 cycles at 0.5 C under a high sulfur loading of 4.4 mg cm^{-2} and an electrolyte-to-sulfur ratio of 6 μL mg^{-1}. In another work, Hou et al.[89] successfully investigated the catalytic mechanism of oxygen vacancies by taking perovskites $Sr_{0.9}Ti_{1-x}Mn_xO_{3-\delta}$ ($STMn_x$, x=0.1−0.3) with various concentrations of OVs as study objects. The effects of OVs on the electronic properties and redox kinetics were researched systematically based on the results of DFT and advanced in-situ experiments. Compared with pristine STO_3, the band gap between p-band center and d-band center decreased

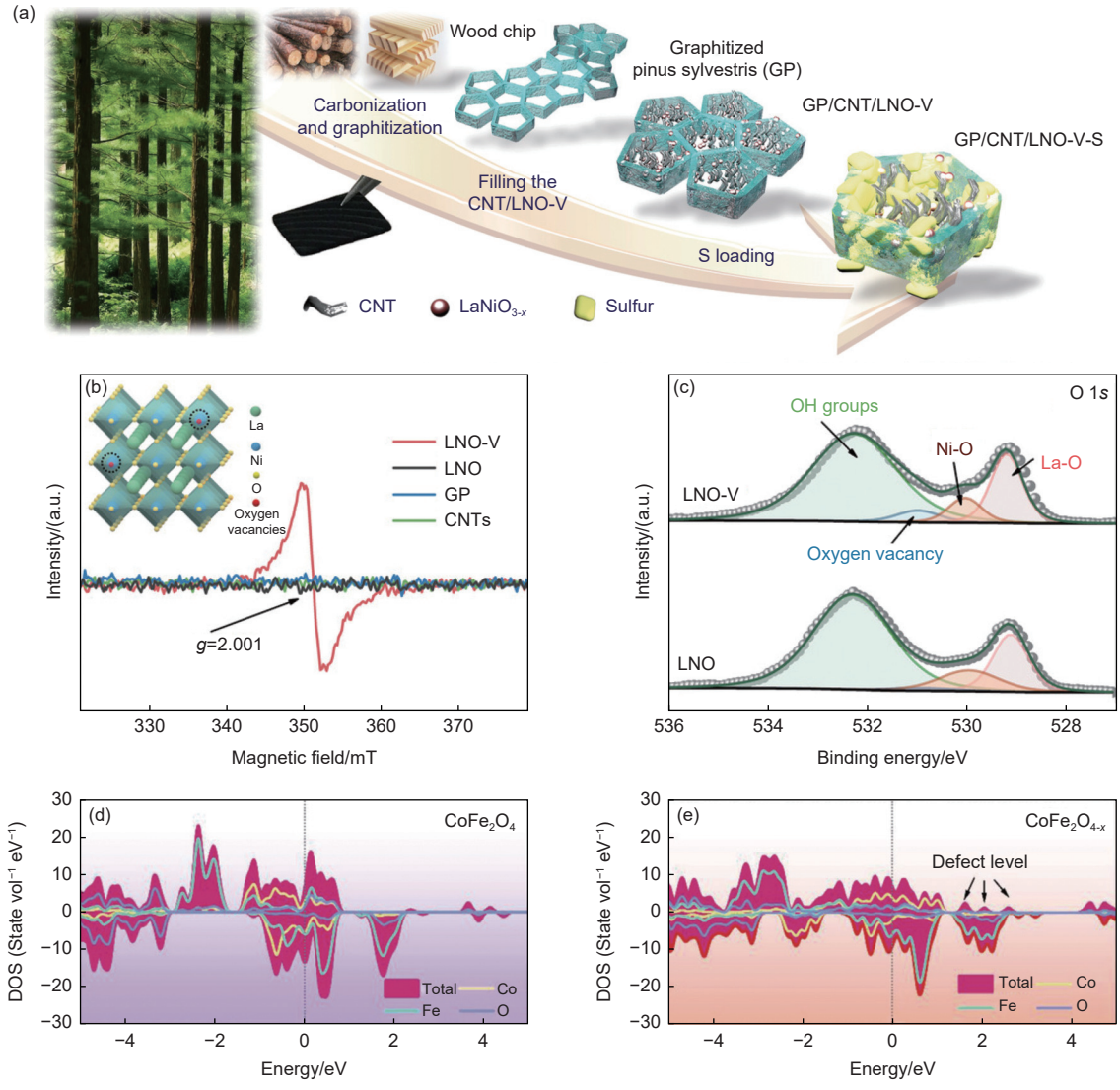

Fig. 7 (a) Schematic illustration of fabrication process of GP/CNT/LNO-V-S nanocomposite[88]. (b) EPR spectra of LNO-V, LNO, GP and CNTs[91]. (c) O 1s XPS spectra of LNO-V and LNO[88]. (d-e) PDOS diagram of $CoFe_2O_4$ and $CoFe_2O_{4-x}$ composite materials[90]. Reproduced with permission

with the incorporation of OVs, which was beneficial to the improvement of electrical conductivity. In addition, in-situ Raman, and in-situ XRD characterization were performed to monitor the real-time changes of LiPSs during charge and discharge process, which demonstrated the increased binding ability of $STMn_{0.3}$ with LiPSs and accelerated redox transformation of LiPSs compared with STO_3.

Generally, the pyrolysis treatment of TMOs-CM to introduce OVs tend to be strict under reducing atmospheres like H_2, CO and NH_3 (or vacuum). Toward this, Hu et al.[90] developed a novel strategy to introduce OVs into NFB $CoFe_2O_{4-x}$ on multiwalled carbon nanotubes (MWCNTs) by using ionic liquids as dopants through a simple solvothermal method. Since new peaks appeared near Fermi level according to the PDOS simulated by DFT calculation (Fig. 7d-e), the electrical conductivity could be greatly enhanced by the abundant OVs in composite material compared with $CoFe_2O_4$@MWCNT without OVs. Due to advantages of excellent trapping ability and promoted deposition of Li_2S, the as-obtained NFB-$CoFe_2O_{4-x}$@MWCNTs enriched in OVs delivered a superior capacity of 870 mAh g^{-1} after 1 000 cycles at 1 C with an extremely low decay rate of 0.016% per cycle.

4.3 Facet manipulation

Since the "adsorption-diffusion-conversion" process tends to take place on the surface of electrode composite during charge and discharge process, the electrochemical performance of Li-S batteries is closely related to the surface structure of the material. Crystal facets exposed on the electrode composite can be modulated to exhibit different surface atomic configuration and coordination environment, resulting in various surface properties and electronic structure, which effectively facilitate the adsorption and catalytic conversion of LiPSs[91–93]. Most of current studies have focused on enhancing the electrocatalytic activity of Li-S batteries through component optimization and structural design, while the electrochemical effect of the crystal surface structure with different atomic arrangements has rarely been studied. Therefore, it provides a feasible and attractive approach to explore the structure-relationship between the crystal facets and electrochemical performance, and accelerate redox kinetics in Li-S batteries by precisely adjusting the exposure of crystal surface facets.

In a recent work, Xiao et al.[94] prepared Co_3O_4-NC (001) and Co_3O_4-NP (112) with various oxidation state of cobalt through crystal structure engineering to regulate the adsorption and catalytic conversion for LiPSs. As compared to Co_3O_4-NC crystals with (001) facet, the Co_3O_4-NP (112) crystals with abundant Co^{3+} active sites presented stronger adsorption and faster catalytic kinetics for LiPSs transformation. Besides, N-rGO as an efficient support could effectively help the growth of Co_3O_4 crystals and improve the overall electronic conductivity. To gain further understanding of the kinetics improvement through crystal facet manipulation, DFT calculations were performed to investigate the Li^+ diffusion path and Li_2S decomposition behavior. As illustrated in Fig. 8a, the Li^+ diffusion barrier and Li_2S decomposition barrier of Co_3O_4 (112) were much lower than those of Co_3O_4 (001), indicating the faster Li^+ transport and promoted Li_2S conversion ability by exposing abundant Co^{3+} active sites. After adsorbing Li_2S_6 intermediates, a higher electron distribution near Fermi level was detected in Co_3O_4 (112) compared with Co_3O_4 (001), indicating stronger chemical interaction with polysulfide intermediates, higher electronic conductivity and boosted redox reaction (Fig. 8b). As a result, the assembled batteries presented a low-capacity decay rate of 0.058% at 1 C after 500 cycles and delivered 4.1 mAh cm^{-2} at 0.1 C with a sulfur loading of 5 mg cm^{-2} and a low E/S ratio of 5.3 mL g^{-1} (Fig. 8c).

Exploring the relationship between crystal surface structure and activity is essential to understand the reaction mechanism and rationally design TMOs-CM electrode materials via facets manipulation. In this sense, Jiang et al.[95] synthesized SnO_2 (332) and SnO_2 (111) crystals on rGO by a facile hydrothermal method through crystal facets engineering. To provide further insight into the electronic structure of the SnO_2 (332) and SnO_2 (111) nanocrystals, it was found that

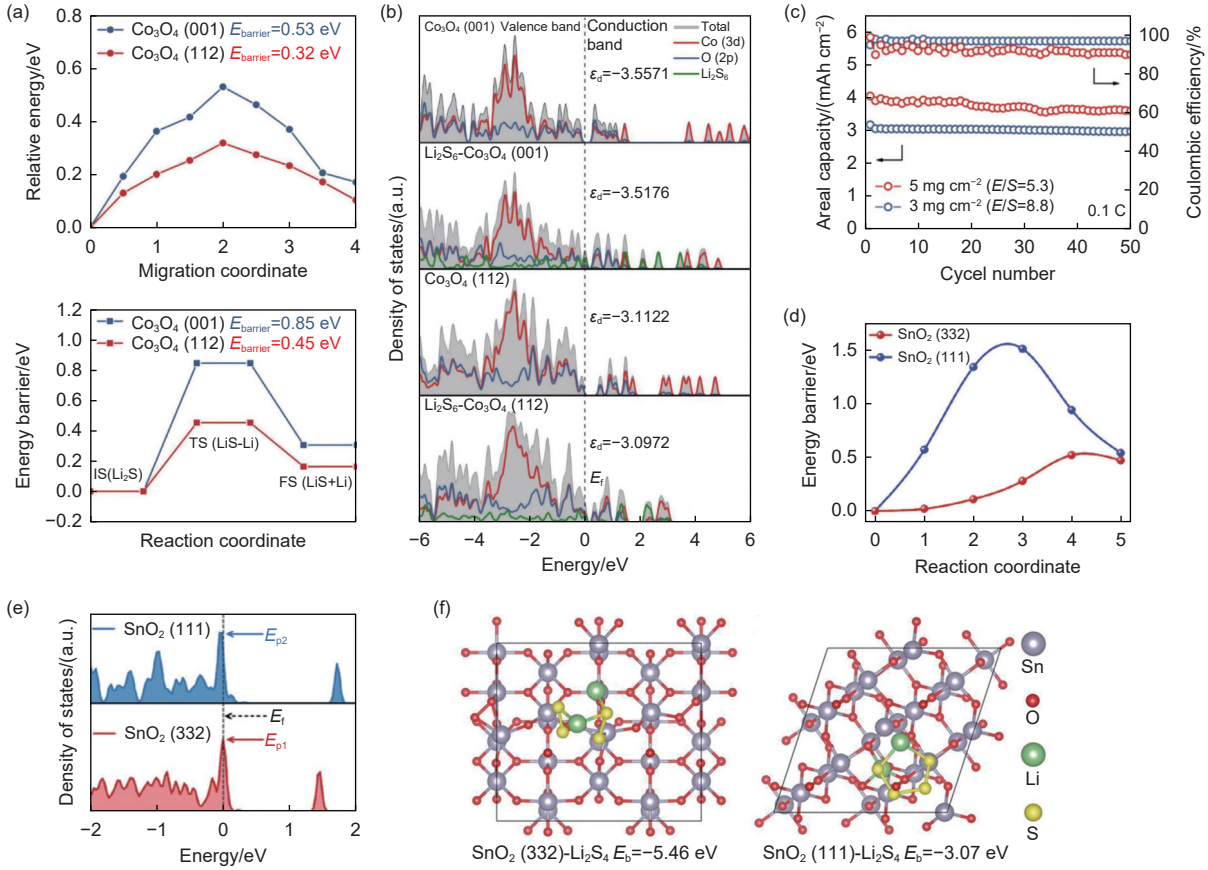

Fig. 8 (a) Li^+ Diffusion profiles and Li_2S decomposition energy profiles on different Co_3O_4 crystal surfaces[94]. (b) Density of status of Co_3O_4 and Li_2S_6-Co_3O_4 with different crystal facets[94]. (c) Cycling performance of S@Co_3O_4-NP/N-rGO at 0.1 C under a high sulfur loading and a low *E*/*S* ratio[94]. (d) Li_2S decomposition energy barriers on surfaces of SnO_2(332) and SnO_2(111)[95]. (e) DOS of Sn atoms on different SnO_2 crystal facets[95]. (f) Binding energy between Li_2S and different SnO_2 crystal facets[95]. Reproduced with permission

SnO_2 with full exposure of high-index (332) facet possessed abundant unsaturated Sn sites according to density of states, demonstrating stronger affinity for LiPSs compared with SnO_2 enclosed by the (111) facets. The interaction between SnO_2 facets and Li_2S was further investigated by DFT calculations. Noteworthy, the decomposition energy barrier of Li_2S on high-index SnO_2 (332) facets were much lower than those on SnO_2 (111) facets, indicating a stronger catalytic ability for the liquid-solid and solid-liquid transformation during repeated cycling. In addition, SnO_2 (332) facets (4.97 eV) could strongly bind with Li_2S compared with SnO_2 (111) facets (3.61 eV), contributing to the uniform deposition of Li_2S and a high sulfur utilization (Fig. 8d-f). As a result, a long-term cycling capacity of 432 mAh g^{-1} was achieved after 2 000 cycles at 2 C with a decay rate of 0.021% with respect to SnO_2 (332) electrode material.

5 Conclusion and outlook

Overall, the regulation of TMOs-CM is regarded as one of the most effective methods to improve long-term cycle stability and rate capacity due to its effectiveness in anchoring LiPSs and promoting catalytic conversion. Therefore, through an integration of the synthesis methods, structural constructions, and modulation strategies of TMOs-CM, rational design principle of electrocatalysts is proposed: (1) Production cost is one of the most important indicators for the practical commercialization of lithium-sulfur batteries, including raw materials and preparation methods. In the field of Li-S batteries, the addition of metal compounds has proved to be an efficient approach to remarkably improve the electrochemical performance. Among various metal compounds (nitrides, phosphides and carbides, etc.), low-cost metal oxides with good stability are recommended since they can be eas-

ily synthesized and further employed in the design of various types of heterostructures, vacancies and facets to alleviate the sluggish LiPSs redox kinetics. Moreover, it is worth noting that the proportion of metal compounds needs to be strictly controlled since an inappropriate content may not only reduce the energy density and cycling life of the cells, but also increase the manufacturing cost of composite materials. (2) Carbon materials have long been considered as excellent supports for metal compounds and efficient physical barriers for LiPSs shuttling. Specifically, in the design of conductive carbon substrates, it is necessary to have abundant conductive channels for rapid electron transfer, large specific surface area for well-distributed metal oxides and hierarchically porous structure for reliable sulfur accommodation and LiPSs confinement. (3) The combination of physical confinement and smooth "adsorption-catalysis" process has proven to be one of the most promising approaches to realize desirable electrochemical performance of Li-S batteries. Modulation strategies, such as heterostructure design, vacancy engineering and facet manipulation, can be employed to inhibit severe shuttle effect and improve sulfur utilization. Specifically, for heterojunction materials, through a synergy of strong adsorption ability of one component and rapid catalytic conversion ability of another one, a smooth "adsorption-diffusion-conversion" process can be realized to greatly promote the electrochemical performance of Li-S batteries. In addition, the adsorption-catalysis ability of the materials can be further enhanced since heterostucture engineering has great operability in material design and optimization. For TMOs-CM with abundant oxygen vacancies, active electrons dispersed around oxygen vacancies in metal oxides can improve the conductivity of composites, while the abundant defect sites contribute to strong affinity and accelerated redox conversion for soluble polysulfides. As for facet manipulation, precise adjustment of crystal facets exposed on TMO-CM composites can present different atomic densities and arrangements, thus facilitating the adsorption and catalytic ability for LiPSs.

Despite remarkable progress of Li-S batteries in recent years, some huge challenges remain to be solved. Firstly, much more attention should be paid to the design of multifunctional composite materials. For the material construction aiming for multifunctional applications, the focus should be directed towards achieving excellent electron/ion conductivity, strong chemical affinity for LiPSs, high redox ability to promote catalytic kinetics and homogeneous Li plating/stripping process. The as-prepared "two-in-one" or "two birds with one stone" electrode materials with superior sulfiphilicity and lithiophilicity could achieve a smooth "adsorption-diffusion-catalysis" process at the cathode side and inhibit lithium dendrite growth at the anode side when applied as sulfur hosts or modified separators to realize excellent electrochemical performance and long cycling life of Li-S batteries.

In addition, the application in scaled-up pouch cell should be emphasized to promote the large-scale commercialization of Li-S batteries. At present, large amounts of electrode materials are employed in coin-type Li-S batteries at a limited lab level, but always achieve a rapid failure when applied in Ah-level pouch cell. Under the condition of practical pouch cells, the shuttling effect, uneven dendrite growth, serious anode corrosion, unstable SEI films and the side reaction between shuttling LiPSs and metal lithium will become more serious, which greatly reduce the energy density and cycling life. Meanwhile, the requirement of wide-temperature range of Li-S cells under extreme temperature conditions (too high or too low temperature) is also urgent. Therefore, the assembled batteries should be tested under a high sulfur content (> 70%), a low E/S ratio (< 5 μL mg^{-1}) and a high sulfur loading (> 6 mg cm^{-2}) to satisfy the practical requirement of Li-S batteries. Moreover, cells with high safety and wide temperature operation window also need to be further explored to evaluate the electrochemical performance comprehensively.

DFT simulated calculation is one of the most important methods to calculate the researched models in Li-S batteries such as binding energy between TMOs-

CM and soluble LiPSs, decomposition energy barriers of Li_2S and density of states, etc. The identification of active sites by DFT makes it possible to rationally design TMOs-CM with different nanostructures and chemical compositions as efficient electrocatalysts. In addition, although numerous sulfur hosts and modified separators have been developed for Li-S batteries, the specific mechanism of its complicated reaction needs to be further investigated. Compared with conventional experimental methods, advanced characterization techniques, such as in-situ Raman, XAS, in-situ XRD, in-situ TEM, etc. can be employed to build a deeper understanding of the structural evolution of catalysts, the property changes of adsorption and catalytic sites during the charge and discharge process and specific redox/interaction mechanism between electrocatalysts and LiPSs.

In summary, the development of TMOs-CM with tunable structural properties and high adsorption-catalytic ability is believed to be one of the most promising strategies for high-performance Li-S batteries. We hope this review can provide some insights regarding the modulation of TMOs-CM to promote the commercial development of Li-S batteries.

Acknowledgements

This work is partly supported by the National Natural Science Foundation of China (U21A2060, 22178116, 21978097), Shanghai Pujiang Program (21PJD019), Natural Science Foundation of Shanghai (22ZR1417400) and the Fundamental Research Funds for the Central Universities (222201817001, 50321041918013, JKA01221601).

References

[1] Geng H Y, Peng Y, Qu L T, et al. Structure design and composition engineering of carbon-based nanomaterials for lithium energy storage[J]. Advanced Energy Materials, 2020, 10(10): 1903030.

[2] Zhao M, Li B Q, Peng H J, et al. Lithium-sulfur batteries under lean electrolyte conditions: challenges and opportunities[J]. Angew Chemie-International Edition, 2020, 59(31): 12636-12652.

[3] Yu X L, Yin Y, Ma C, et al. N-doped porous carbon@CNT nanowire as effective polysulfides adsorption-catalysis interlayer for high-performance lithium-sulfur batteries[J]. Chemical Engineering Science, 2023, 268: 118400.

[4] Tan S Y, Wu Y F, Kan S T, et al. A combination of MnO_2-decorated graphene aerogel modified separator and I/N codoped graphene aerogel sulfur host to synergistically promote Li-S battery performance[J]. Electrochimica Acta, 2020, 348: 136173.

[5] Fang R P, Chen K, Yin L C, et al. The regulating role of carbon nanotubes and graphene in lithium-ion and lithium-sulfur batteries[J]. Advanced Materials, 2019, 31(9): 1800863.

[6] Yuan C, Yang X F, Zeng P, et al. Recent progress of functional separators with catalytic effects for high-performance lithium- sulfur batteries[J]. Nano Energy, 2021, 84: 105928.

[7] Wang T, He J R, Cheng X B, et al. Strategies toward high-loading lithium-sulfur batteries[J]. ACS Energy Letters, 2022, 8(1): 116-150.

[8] Wu J, Ye T, Wang Y C, et al. Understanding the catalytic kinetics of polysulfide redox reactions on transition metal compounds in Li-S batteries[J]. ACS Nano, 2022, 16(10): 15734-15759.

[9] Lim W G, Kim S, Jo C, et al. A comprehensive review of materials with catalytic effects in Li-S batteries: Enhanced redox kinetics[J]. Angewandte Chemie International Edition, 2019, 58(52): 18746-18757.

[10] Yao W Q, Xu J, Ma L B, et al. Recent progress for concurrent realization of shuttle-inhibition and dendrite-free lithium-sulfur batteries[J]. Advanced Materials, 2023, 35: 2212116.

[11] Chung S H, Manthiram A. Current status and future prospects of metal-sulfur batteries[J]. Advanced Materials, 2019, 31(27): 1901125.

[12] Zeng P, Su B, Wang X L, et al. In situ reconstruction of electrocatalysts for lithium-sulfur batteries: Progress and prospects[J]. Advanced Functional Materials, 2023, 33: 2301743.

[13] Song Y Z, Cai W L, Kong L, et al. Rationalizing electrocatalysis of Li-S chemistry by mediator design: Progress and prospects[J]. Advanced Energy Materials, 2019, 10(11): 1901075.

[14] Ng S F, Lau M Y L, Ong W J. Lithium-sulfur battery cathode design: tailoring metal-based nanostructures for robust polysulfide adsorption and catalytic conversion[J]. Advanced Materials, 2021, 33(50): 2008654.

[15] Liu Y T, Liu S, Li G R, et al. Strategy of enhancing the volumetric energy eensity for lithium-sulfur batteries[J]. Advanced Materials, 2021, 33(8): 2003955.

[16] Li S L, Zhang W F, Zheng J F, et al. Inhibition of polysulfide shuttles in Li-S batteries: Modified separators and solid-state electrolytes[J]. Advanced Energy Materials, 2020, 11(2): 2000779.

[17] Huang Y Z, Lin L, Zhang C K, et al. Recent advances and strategies toward polysulfides shuttle inhibition for high- performance Li-S batteries[J]. Advanced Science, 2022, 9(12): 2106004.

[18] David L, Bhandavat R, Gurpreet Singh. MoS_2/graphene composite paper for sodium-ion battery electrodes[J]. ACS Nano, 2014, 8(2): 1759-1770.

[19] Yu L Q, Zhao S X, Wu Q L, et al. Strengthening the interface between flower-like VS_4 and porous carbon for improving its lithium storage performance[J]. Advanced Functional Materials, 2020, 30(16): 2000427.

[20] Song Z R, Zhang G Y, Deng X L, et al. Strongly coupled interfacial engineering inspired by robotic arms enable high-performance sodium-ion capacitors[J]. Advanced Functional Materials, 2022, 32(38): 2205453.

[21] Wang J M, Wang B B, Liu X J, et al. Prussian blue analogs (PBA) derived porous bimetal (Mn, Fe) selenide with carbon nanotubes as anode materials for sodium and potassium ion batteries[J]. Chemical Engineering Journal, 2020, 382: 123050.

[22] Ruan S J, Luo D, Li M, et al. Synthesis and functionalization of 2D nanomaterials for application in lithium-based energy storage systems[J]. Energy Storage Materials, 2021, 38: 200-230.

[23] Li S, Cen Y, Xiang Q, et al. Vanadium dioxide-reduced graphene oxide binary host as an efficient polysulfide plague for high-performance lithium-sulfur batteries[J]. Journal of Materials Chemistry A, 2019, 7(4): 1658-1668.

[24] Ding M, Huang S Z, Wang Y, et al. Promoting polysulfide conversion by catalytic ternary Fe_3O_4/carbon/graphene composites with ordered microchannels for ultrahigh-rate lithium-sulfur batteries[J]. Journal of Materials Chemistry A, 2019, 7(43): 25078-25087.

[25] Li Z, Zhang F, Cao T, et al. Highly stable lithium-sulfur batteries achieved by a SnS/porous carbon nanosheet architecture modified Celgard separator[J]. Advanced Functional Materials, 2020, 30(48): 2006297.

[26] Liu L, Li Y K, Zhang Y G, et al. CoP@C with chemisorption-catalysis effect toward lithium polysulfides as multifunctional interlayer for high-performance lithium-sulfur batteries[J]. Electrochimica Acta, 2022, 419: 140391.

[27] Qiao S M, Wang Q, Zhang Q, et al. Sacrificial template method to synthesize atomically dispersed Mn atoms on S, N-codoped carbon as a separator modifier for advanced Li-S batteries[J]. ACS Applied Materials & Interfaces, 2022, 14(37): 42123-42133.

[28] Salhabi E H M, Zhao J L, Wang J Y, et al. Hollow multi-shelled structural TiO_{2-x} with multiple spatial confinement for long-life lithium-sulfur batteries[J]. Angewandte Chemie-International Edition, 2019, 58(27): 9078-9082.

[29] Lin Y, Li J C, Xie W J, et al. FeCoNi ternary nano-alloys embedded in a nitrogen-doped porous carbon matrix with enhanced electrocatalysis for stable lithium-sulfur batteries[J]. ACS Applied Materials & Interfaces, 2022, 14(45): 51001-51009.

[30] Han X G, Xu Y H, Chen X Y, et al. Reactivation of dissolved polysulfides in Li-S batteries based on atomic layer deposition of Al_2O_3 in nanoporous carbon cloth[J]. Nano Energy, 2013, 2(6): 1197-1206.

[31] Yi R W, Liu C G, Zhao Y C, et al. A light-weight free-standing graphene foam-based interlayer towards improved Li-S cells[J]. Electrochimica Acta, 2019, 299: 479-488.

[32] Wang B, Ruan T T, Chen Y, et al. Graphene-based composites for electrochemical energy storage[J]. Energy Storage Materials, 2020, 24: 22-51.

[33] Kong Z K, Li Y, Wang Y L, et al. Monodispersed MnO_x-CeO_2 solid solution as superior electrocatalyst for Li_2S precipitation and conversion[J]. Chemical Engineering Journal, 2020, 392: 123697.

[34] Ni L B, Duan S Q, Zhang H Y, et al. A 3D Graphene/WO_3 nanowire composite with enhanced capture and polysulfides conversion catalysis for high-performance Li-S batteries[J]. Carbon, 2021, 182: 335-347.

[35] Chen M H, Li T Y, Li Y, et al. Rational design of a MnO nanoparticle-embedded carbon nanofiber interlayer for advanced lithium-sulfur batteries[J]. ACS Applied Energy Materials, 2020, 3(11): 10793-10801.

[36] Yang R L, Du H W, Lin Z Q, et al. ZnO nanoparticles filled tetrapod-shaped carbon shell for lithium-sulfur batteries[J]. Carbon, 2019, 141: 258-265.

[37] Luo Y H, Ouyang Z Y, Lin Y, et al. Revealing the synergistic mechanism of multiply nanostructured V_2O_3 hollow nanospheres integrated with doped N, Ni heteroatoms, in-situ grown carbon nanotubes and coated carbon nanolayers for the enhancement of lithium-sulfur batteries[J]. Journal of Colloid and Interface Science, 2022, 612: 760-771.

[38] Sun Q, Cheng X M, Ma C, et al. NiSe nanoparticles decorated corn stalk derived 2D carbon nanosheet as separator modifier for high-performance lithium-sulfur batteries[J]. Journal of Power Sources, 2023, 585: 233645.

[39] Yao W Q, Tian C X, Yang C, et al. P-doped $NiTe_2$ with Te-vacancies in lithium-sulfur batteries prevents shuttling and promotes polysulfide conversion[J]. Advanced Materials, 2022, 34(11): 2106370.

[40] Sun R, Bai Y, Bai Z, et al. Phosphorus vacancies as effective polysulfide promoter for high-energy-density lithium-sulfur batteries[J]. Advanced Energy Materials, 2022, 12(12): 2102739.

[41] Ruan S J, Huang Z C, Cai W D, et al. Enabling rapid polysulfide conversion kinetics by using functionalized carbon nanosheets as metal-free electrocatalysts in durable lithium-sulfur batteries[J]. Chemical Engineering Journal, 2020, 385: 123840.

[42] Ma C, Zheng Z F, Jia X F, et al. Promoting the synergistic effect of sulfur immobilization and polysulfides trapping by nitrogen functionalized interconnected hollow carbon nanocages for high-performance lithium-sulfur batteries[J]. Journal of Power Sources, 2021, 486: 229358.

[43] Fu C Y, Oviedo M B, Zhu Y H, et al. Confined lithium-sulfur reactions in narrow-diameter carbon nanotubes reveal enhanced electrochemical reactivity[J]. ACS Nano, 2018, 12(10): 9775-9784.

[44] Choi C, Lee D Y, Park J B, et al. Separators modified using MoO_2@carbon nanotube nanocomposites as dual-mode Li-

polysulfide anchoring materials for high-performance anti-self-discharge lithium-sulfur batteries[J]. ACS Sustainable Chemistry & Engineering, 2020, 8(40): 15134-15148.

[45] Yao Y, Chang C Y, Li R R, et al. Intrinsic catalytic sites-rich co-doped SnO_2 nanoparticles enabling enhanced conversion and capture of polysulfides[J]. Chemical Engineering Journal, 2022, 431: 134033.

[46] Qiu W L, Li J, Zhang Y G, et al. Carbon nanotubes assembled on porous TiO_2 matrix doped with Co_3O_4 as sulfur host for lithium-sulfur batteries[J]. Nanotechnology, 2021, 32(7): 075403.

[47] Wen G Y, Zhang X P, Shi Z H, et al. Sphere-in-fiber hybrid of N-doped carbon/cerium dioxide as an interlayer material with superior electrocatalytic performance for lithium sulfide precipitation and conversion[J]. Journal of Colloid and Interface Science, 2022, 619: 106-115.

[48] Saroha R, Oh J H, Lee J S, et al. Hierarchically porous nanofibers comprising multiple core-shell Co_3O_4@graphitic carbon nanoparticles grafted within N-doped CNTs as functional interlayers for excellent Li-S batteries[J]. Chemical Engineering Journal, 2021, 426: 130805.

[49] Zhang H J, Liu Q Z, Ruan S J, et al. In-situ construction of g-C_3N_4/carbon heterostructure on graphene nanosheet: an efficient polysulfide barrier for advanced lithium-sulfur batteries[J]. Applied Surface Science, 2022, 578: 152022.

[50] He X M, Li B J, Lei Z H, et al. Multifunctional effects of hollow flower-like $CoTiO_3$ microspheres wrapped by reduced graphene as sulfur host in Li-S battery[J]. Journal of Colloid and Interface Science, 2022, 626: 963-974.

[51] Qiu P P, Yao Y, Li W, et al. Sub-nanometric manganous oxide clusters in nitrogen doped mesoporous carbon nanosheets for high-performance lithium-sulfur batteries[J]. Nano Letters, 2021, 21(1): 700-708.

[52] Li Y L, Zhang X F, Zhang Q, et al. Layer-by-Layer assembly of CeO_{2-x}@C-rGO nanocomposites and CNTs as a multifunctional separator coating for highly stable lithium-sulfur batteries[J]. ACS Applied Materials & Interfaces, 2022, 14(16): 18634-18645.

[53] Jian Z X, Zhang S C, Guan X G, et al. ZnO quantum dot-modified rGO with enhanced electrochemical performance for lithium- sulfur batteries[J]. RSC Advances, 2020, 10(54): 32966-32975.

[54] Guo R T, Li W, Huang R Q, et al. Shuttle-inhibited 3D sandwich MXene/SnO_2 QDs sulfur host for high-performance lithium-sulfur batteries[J]. Journal of Alloys and Compounds, 2023, 937: 168427.

[55] Seon Y H, Saroha R, Cho J S. Hierarchically porous N-doped C nanofibers comprising TiO_2 quantum dots and ZIF-8-derived hollow C nanocages as ultralight interlayer for stable Li-S batteries[J]. Composites Part B:Engineering, 2022, 237: 109856.

[56] Zhang H, Yang L, Zhang P G, et al. MXene-derived Ti_nO_{2n-1} quantum dots distributed on porous carbon nanosheets for stable and long-life Li-S Batteries: Enhanced polysulfide mediation via defect engineering[J]. Advanced Materials, 2021, 33(21): 2008447.

[57] Yang L B, Wang X W, Cheng X M, et al. Regulating Fe aggregation state via unique Fe–N–V pre-coordination to optimize the adsorption-catalysis effect in high-performance lithium-sulfur batteries[J]. Advanced Functional Materials, 2023, 33: 2303705.

[58] Li X Y, Han Z Y, Yang W H, et al. 3D ordered porous hybrid of ZnSe/N-doped carbon with anomalously high Na^+ mobility and ultrathin solid electrolyte interphase for sodium-ion batteries[J]. Advanced Functional Materials, 2021, 31(50): 2106194.

[59] Cheng H, Zhang S C, Li S Y, et al. Engineering Fe and V coordinated bimetallic oxide nanocatalyst Enables enhanced polysulfides mediation for high energy density Li-S battery[J]. Small, 2022, 18(28): 2202557.

[60] Wang J Y, Li G R, Luo D, et al. Engineering the conductive network of metal oxide-based sulfur cathode toward efficient and longevous lithium-sulfur batteries[J]. Advanced Energy Materials, 2020, 10(41): 2002076.

[61] Zhu Z J, Yin H J, Wang Y, et al. Coexisting single-atomic Fe and Ni sites on hierarchically ordered porous carbon as a highly efficient ORR electrocatalyst[J]. Advanced Materials, 2020, 32(42): 2004670.

[62] Wei X L, Luo Y H, Du X H, et al. Porous transition metal oxide scaffold implanted with interpenetrated catalytic network enabling polysulfides restricted and dendrite free lithium-sulfur batteries[J]. Chemical Engineering Journal, 2023, 454: 140152.

[63] Xu C, Zheng S N, Guo J, et al. Cobalt-loaded three-dimensional ordered Ta/N-doped TiO_2 framework as conductive multi-functional host for lithium-sulfur battery[J]. Chemical Engineering Journal, 2023, 463: 142295.

[64] Liu Y, Ma Z Y, Yang G, et al. Multifunctional $ZnCo_2O_4$ quantum dots encapsulated in carbon carrier for anchoring/catalyzing polysulfides and self-repairing lithium metal anode in lithium-Sulfur Batteries[J]. Advanced Functional Materials, 2021, 32(12): 2109462.

[65] Liang X, Hart C, Pang Q, et al. A highly efficient polysulfide mediator for lithium-sulfur batteries[J]. Nature Communications, 2015, 6: 5682.

[66] Shao Q J, Guo D C, Wang C, et al. Yolk-shell structure MnO_2@Hollow carbon nanospheres as sulfur host with synergistic encapsulation of polysulfides for improved Li-S batteries[J]. Journal of Alloys and Compounds, 2020, 842: 155790.

[67] Zhang Y, Ma L, Tang R X, et al. Hollow carbon nanospheres coated by δ-MnO_2 as S host to enhance the catalytic conversion of polysulfides in Li-S batteries[J]. Applied Surface Science, 2022, 585: 152498.

[68] Ji M Z, Ni J, Liang X, et al. Biomimetic synthesis of VO_x@C yolk-shell nanospheres and their application in Li-S Batteries[J]. Advanced Functional Materials, 2022, 32(48): 2206589.

[69] Zhang Y Z, Ge X, Kang Q, et al. Vanadium oxide nanorods embed in porous graphene aerogel as high-efficiency polysulfide-trapping -

conversion mediator for high performance lithium-sulfur batteries[J]. Chemical Engineering Journal, 2020, 393: 124570.

[70] Wang M, Tan S Y, Kan S T, et al. In-situ assembly of TiO_2 with high exposure of (001) facets on three-dimensional porous graphene aerogel for lithium-sulfur battery[J]. Journal of Energy Chemistry, 2020, 49: 316-322.

[71] Chang Z, Dou H, Ding B, et al. Co_3O_4 nanoneedle arrays as a multifunctional "super-reservoir" electrode for long cycle life Li-S batteries[J]. Journal of Materials Chemistry A, 2017, 5(1): 250-257.

[72] Chen S J, Zhang J X, Wang Z Y, et al. Electrocatalytic $NiCo_2O_4$ nanofiber arrays on carbon cloth for flexible and high-loading Lithium-Sulfur Batteries[J]. Nano Letters, 2021, 21(12): 5285-5292.

[73] Yao L, Dong X W, Zhang C R, et al. Metal oxide nanoprism-arrays assembled in N-doped carbon foamy nanoplates that have efficient polysulfide-retention for ultralong-cycle-life lithium-sulfur batteries[J]. Journal of Materials Chemistry A, 2018, 6(24): 11260-11269.

[74] Chu R R, Nguyen T T, Bai Y Q, et al. Uniformly controlled treble boundary using enriched adsorption sites and accelerated catalyst cathode for robust lithium-sulfur batteries[J]. Advanced Energy Materials, 2022, 12(9): 2102805.

[75] Sun J M, Liu Y H, Bi J X, et al. Interface engineering toward expedited Li_2S deposition in lithium –sulfur batteries: A critical review[J]. Advanced Materials, 2023, 35: 2211168.

[76] Deng S G, Guo T Z, Heier J, et al. Unraveling polysulfide's adsorption and electrocatalytic conversion on metal oxides for Li-S batteries[J]. Advanced Science, 2023, 10(5): 2204930.

[77] Zhao X, Liu M J, Wang Y C, et al. Designing a built-in electric field for efficient energy electrocatalysis[J]. ACS Nano, 2022, 16(12): 19959-19979.

[78] Li Y, Zhang J W, Chen Q G, et al. Emerging of heterostructure materials in energy storage: A Review[J]. Advanced Materials, 2021, 33(27): 2100855.

[79] Cao Z X, Jia J Y, Chen S N, et al. Integrating polar and conductive Fe_2O_3-Fe_3C interface with rapid polysulfide diffusion and conversion for high-performance lithium sulfur batteries[J]. ACS Applies Materials & Interfaces, 2019, 11(43): 39772-39781.

[80] Liang X, Kwok C Y, Lodi-Marzano F, et al. Tuning transition metal oxide-Sulfur interactions for long life lithium sulfur batteries: the "goldilocks " principle[J]. Advanced Energy Materials, 2016, 6(6): 1501636.

[81] Zhang L, Liu Y C, Zhao Z D, et al. Enhanced polysulfide regulation via porous catalytic V_2O_3/V_8C_7 heterostructures derived from metal-organic frameworks toward high- performance Li-S Batteries[J]. ACS Nano, 2020, 14(7): 8495-8507.

[82] Xu Z, Wang Z, Wang M R, et al. Large-scale synthesis of Fe_9S_{10}/Fe_3O_4@C heterostructure as integrated trapping-catalyzing interlayer for highly efficient lithium-sulfur batteries[J]. Chemical Engineering Journal, 2021, 422: 130049.

[83] Lee J, Choi C, Park J B, et al. Optimally arranged TiO_2@MoS_2 heterostructures with effectively induced built-in electric field for high-performance lithium-sulfur batteries[J]. Journal of Energy Chemistry, 2023, 10(83): 496-508.

[84] Yao W Q, Xu J, Cao Y J, et al. Dynamic intercalation-conversion site supported ultrathin 2D mesoporous SnO_2/$SnSe_2$ hybrid as bifunctional polysulfide immobilizer and lithium regulator for lithium-sulfur chemistry[J]. ACS Nano, 2022, 16(7): 10783-10797.

[85] Zhu X R, Zhang X H, Li Y F, et al. Exploring transition metal oxide-based oxygen vacancy supercapacitors: A review[J]. Journal of Energy Storage, 2024, 80: 110350.

[86] Shi Z X, Li M T, Sun J Y, et al. Defect engineering for expediting Li-S chemistry: Strategies, mechanisms, and perspectives[J]. Advanced Energy Materials, 2021, 11(23): 2100332.

[87] Song Y, Li H, Li J F, et al. Rationalizing the impact of oxygen vacancy on polysulfide conversion kinetics for highly efficient lithium-sulfur batteries[J]. Journal of Energy Chemistry, 2023, 87: 51-60.).

[88] Zou K Y, Zhou T F, Chen Y Z, et al. Defect engineering in a multiple confined geometry for robust lithium-sulfur batteries[J]. Advanced Energy Materials, 2022, 12(18): 2103981.

[89] Hou W S, Feng P L, Guo X, et al. Catalytic mechanism of oxygen vacancies in perovskite oxides for lithium-sulfur batteries[J]. Advanced Materials, 2022, 34(26): 2202222.

[90] Hu S Y, Yi M J, Wu H, et al. Ionic-liquid-assisted synthesis of N, F, and B co-doped $CoFe_2O_{4-x}$ on multiwalled carbon nanotubes with enriched oxygen vacancies for Li-S batteries[J]. Advanced Functional Materials, 2021, 32(14): 2111084.

[91] Jiang B, Tian D, Qiu Y, et al. High-index faceted nanocrystals as highly efficient bifunctional electrocatalysts for high-performance lithium-sulfur batteries[J]. Nano-Micro Letters, 2021, 14(1): 40.

[92] Yu Z H, Lv W, Lin Q W, et al. A (110) facet-dominated vanadium dioxide enabling bidirectional electrocatalysis for lithium-sulfur batteries[J]. ACS Nano, 2021, 15(10): 16878-16886.

[93] Wang Z Y, Zhang B, Liu S, et al. Nickel-platinum alloy nanocrystallites with high-index facets as highly effective core catalyst for lithium-sulfur Batteries[J]. Advanced Functional Materials, 2022, 32(27): 2200893.

[94] Xiao R J, Luo D, Wang J Y, et al. Oxidation states regulation of cobalt active sites through crystal surface engineering for enhanced polysulfide conversion in lithium-sulfur batteries[J]. Advanced Science, 2022, 9(31): 2202352.

[95] Jiang B, Qiu Y, Tian D, et al. Crystal facet engineering induced active tin dioxide nanocatalysts for highly stable lithium-sulfur batteries[J]. Advanced Energy Materials, 2021, 11(48): 2102995.

金属氧化物/炭复合材料抑制锂硫电池穿梭效应的研究进展

周志强， 王惠民， 杨璐彬， 马 成， 王际童*， 乔文明， 凌立成*

（华东理工大学 化工学院, 上海 200237）

摘 要： 锂硫电池因理论能量密度高、生产成本低和环境友好等优点被认为是最有前途的下一代电化学储能装置之一。然而，硫和硫化锂的低导电性、严重的穿梭效应和缓慢的反应动力学等问题阻碍了锂硫电池的大规模商业化应用。炭材料因高比表面积，良好导电性与结构多样性而备受关注，然而非极性炭材料难以与极性多硫化物紧密结合，导致活性材料大量损失和严重的穿梭效应。金属氧化物具有极性强和丰富吸附位点的优点，将过渡金属氧化物与炭材料结合，有助于增强对多硫化物的化学吸附和电化学反应活性。本文首先介绍了锂硫电池的基本原理和存在的主要问题，然后讨论了近年来过渡金属氧化物/炭复合材料在合成方法和结构设计（1D，2D，3D）方面的研究进展。此外，详细介绍了异质结构设计、空位工程和晶面调控策略的代表性工作并讨论了其机理。最后，对过渡金属氧化物/炭复合材料用于锂硫电池中的发展进行了总结和展望。

关键词： 过渡金属氧化物；炭材料；调控方案；穿梭效应；锂硫电池

中图分类号： TB33 **文献标识码：** A

通讯作者： 王际童, 教授. E-mail: wangjt@ecust.edu.cn;
凌立成, 教授. E-mail: lchling@ecust.edu.cn

作者简介： 周志强, 博士. E-mail: zhouzhiqianggood@163.com

本文的电子版全文由 Elsevier 出版社在 ScienceDirect 上出版（https://www.sciencedirect.com/journal/new-carbon-materials/）